

Redox-Active Organic Materials: From Energy Storage to Redox Catalysis

Published as part of ACS Materials Au virtual special issue "2023 Rising Stars".

Jaehwan Kim, Jianheng Ling, Yihuan Lai, and Phillip J. Milner*



Cite This: *ACS Mater. Au* 2024, 4, 258–273



Read Online

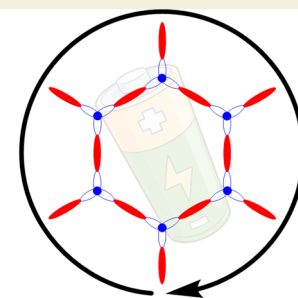
ACCESS |

Metrics & More

Article Recommendations

ABSTRACT: Electroactive materials are central to myriad applications, including energy storage, sensing, and catalysis. Compared to traditional inorganic electrode materials, redox-active organic materials such as porous organic polymers (POPs) and covalent organic frameworks (COFs) are emerging as promising alternatives due to their structural tunability, flexibility, sustainability, and compatibility with a range of electrolytes. Herein, we discuss the challenges and opportunities available for the use of redox-active organic materials in organoelectrochemistry, an emerging area in fine chemical synthesis. In particular, we highlight the utility of organic electrode materials in photoredox catalysis, electrochemical energy storage, and electrocatalysis and point to new directions needed to unlock their potential utility for organic synthesis. This Perspective aims to bring together the organic, electrochemistry, and polymer communities to design new heterogeneous electrocatalysts for the sustainable synthesis of complex molecules.

KEYWORDS: redox-active, organic materials, electrocatalysis, photocatalysis, electrochemistry porous organic polymers, covalent organic frameworks



Redox-Active Organic Materials

Energy storage · Photoredox · Electrocatalysis

1. INTRODUCTION

Electrochemistry is vital to energy storage, chemical manufacturing, separations, sensing, and beyond.^{1–4} Over the past decade, electrochemistry has (re)emerged as a powerful tool for the synthesis of complex molecules as well.^{5–9} The key advantages offered by organic electrosynthesis include access to novel reactivity patterns, waste reduction, safety, scalability, and sustainability.¹⁰ Similar to photoredox catalysis, electro-synthesis facilitates retrosynthetic disconnections based on single electron transfer (SET) that are difficult to replicate using traditional two-electron logic.^{11,12} As such, countless new electrochemical synthetic methodologies are being developed, changing the way we make organic molecules relevant to the pharmaceutical and fine chemical industries.

Most electrochemical transformations proceed via electron transfer to/from the substrate at an electrode surface. However, organic molecules tend to interact poorly with the surfaces of common electrode materials, slowing the kinetics of such direct electrolysis reactions and leading to undesirable side reactions.¹³ To overcome these limitations, molecular catalysts that shuttle electrons between the substrate and electrode—referred to as redox mediators—have been developed to enable the functionalization of inert substrates such as unactivated haloarenes.^{13–16} This approach is termed indirect electrolysis. The vast majority of such mediators are homogeneous, which decreases their stability, scalability, and

recyclability. Molecular redox mediators or electrocatalysts can be grafted to electrode surfaces to overcome some of these drawbacks.^{16–18} However, immobilized mediators remain underutilized in organic electrosynthesis, likely due to challenges associated with their preparation, characterization, and reliable attachment to electrode surfaces.

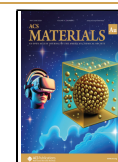
Inorganic solids currently dominate applications in electrochemistry, such as for secondary batteries and supercapacitors.¹⁹ However, traditional inorganic electrode materials such as LiCoO_2 suffer from several key challenges, including high processing and mining costs and poor sustainability.²⁰ In recent years, redox-active polymers have emerged as promising alternatives for electrochemical energy storage due to their structural tunability, flexibility, adaptability with a range of charge-compensating ions, high theoretical capacity, and low cost (Figure 1).^{21–25} Organic electrode materials are of particular interest for applications that require fast electrochemical charge/discharge rates, such as in automobiles.²² The major barriers to the wide-scale deployment of organic

Received: November 9, 2023

Revised: December 21, 2023

Accepted: December 22, 2023

Published: January 12, 2024



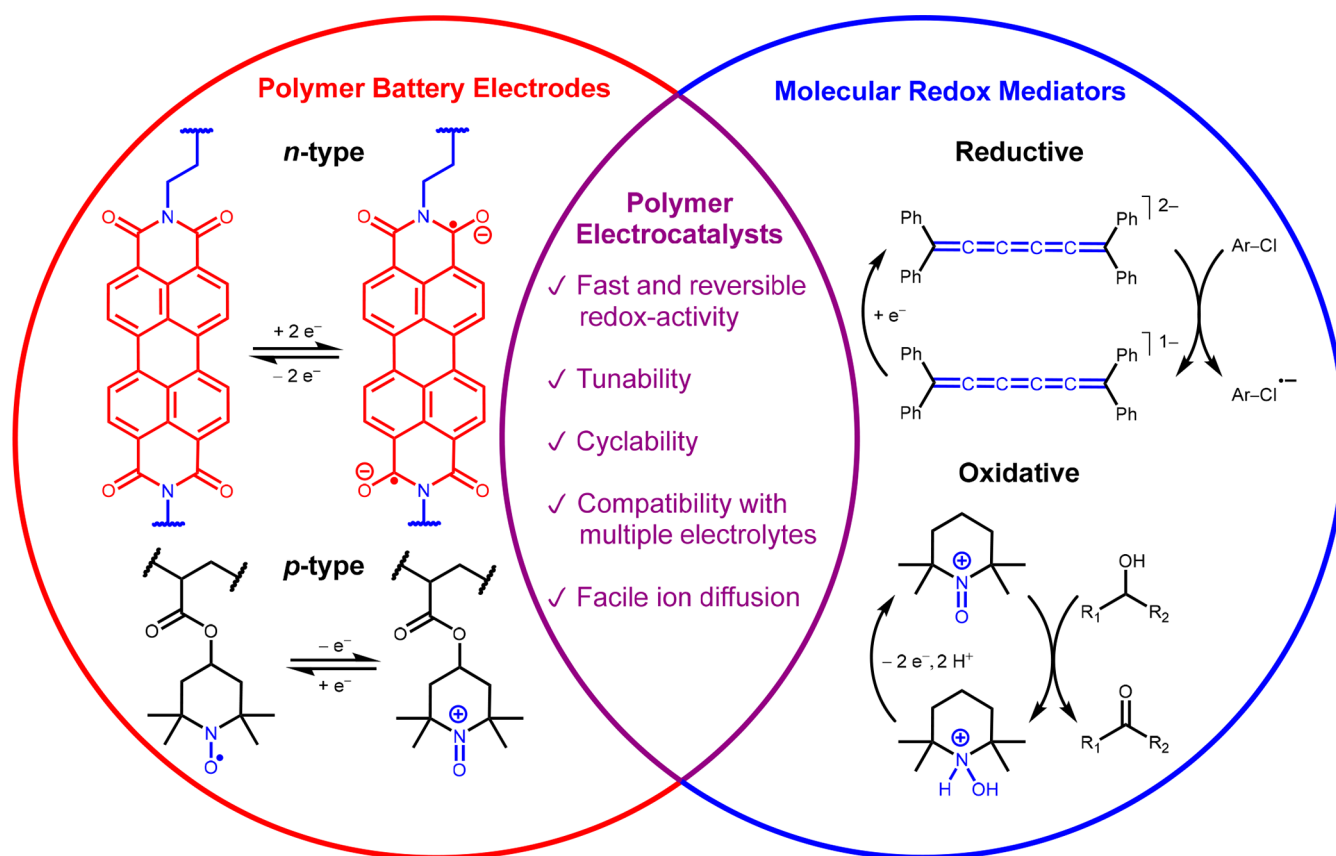


Figure 1. Types of polymer battery electrodes (left), molecular redox mediators (right), and shared desirable traits between the two applications as inspiration for electrocatalysis (middle).

electrode materials are limited cycling stability, dissolution into organic electrolytes, and poor electronic conductivity.^{21,26,27} Nonetheless, emerging structure–property trends are guiding the development of next-generation organic battery materials with improved performance.^{28–31}

Considering the utility of (immobilized) molecular redox mediators in electrocatalysis and of organic electrode materials for electrochemical energy storage, it is surprising that redox-active polymers remain understudied as heterogeneous electrocatalysts for organic synthesis (Figure 1). This gap is particularly notable because redox-active organic materials have been widely studied as photoredox catalysts in organic synthesis^{32–41} and as electrocatalysts in the context of clean energy and sustainability.^{42–48} Herein, we outline the challenges and opportunities available for polymers as heterogeneous redox mediators relevant to organic synthesis, with an emphasis on amorphous porous organic polymers (POPs) and crystalline covalent organic frameworks (COFs).^{49–56} First, we present promising examples of photoredox catalysis with POPs and COFs, focusing on examples in which unique reactivity patterns can be achieved compared to molecular systems (section 2). This discussion highlights the potential of polymeric organic materials to facilitate further redox transformations. Second, we discuss the redox properties of insoluble organic materials, highlighting their promising features compared to traditional inorganic electrode materials (section 3). Last, we highlight desirable features demonstrated by redox-active polymers as electrocatalysts, with CO₂ reduction and alcohol oxidation as representative examples (section 4). We conclude by

discussing future directions for the field (section 5). This Perspective aims to bring together the battery, polymer, organic, and electrochemistry communities to identify new redox-active organic materials suitable for the sustainable production of complex molecules via heterogeneous organic electrocatalysis.

2. PHOTOREDOX CATALYSIS WITH ORGANIC POLYMERS

Photoredox catalysis involves SET between the catalyst and substrate. Thus, drawing inspiration from photoredox catalysis with polymeric materials offers valuable insights into their potential for heterogeneous organoelectrocatalysis as well. The vast majority of photoredox transformations involve homogeneous catalysts,⁵⁷ yet recent work has demonstrated the promise offered by heterogeneous catalysts.³⁸ Heterogeneous photoredox catalysis relevant to energy and environmental applications has been extensively reviewed and is beyond the scope of this Perspective.^{58–64} In this section, we focus on the use of organic materials as heterogeneous photoredox catalysts relevant to organic chemistry.^{32–41}

2.1. POPs as Heterogeneous Photocatalysts

POPs have been widely utilized as heterogeneous photocatalysts in organic transformations, owing to their low cost, structural robustness, high tunability, and good recyclability.^{38,65} Since the seminal work by Lin and co-workers in 2011,⁶⁶ in which photoactive moieties such as [Ru(bpy)₃]²⁺ (bpy = 2,2'-bipyridine) and [Ir(ppy)₂(bpy)]⁺ (ppy = 2-phenylpyridine) were immobilized into cross-linked polymer networks, conjugated polymeric photocatalysts (CPPs) have

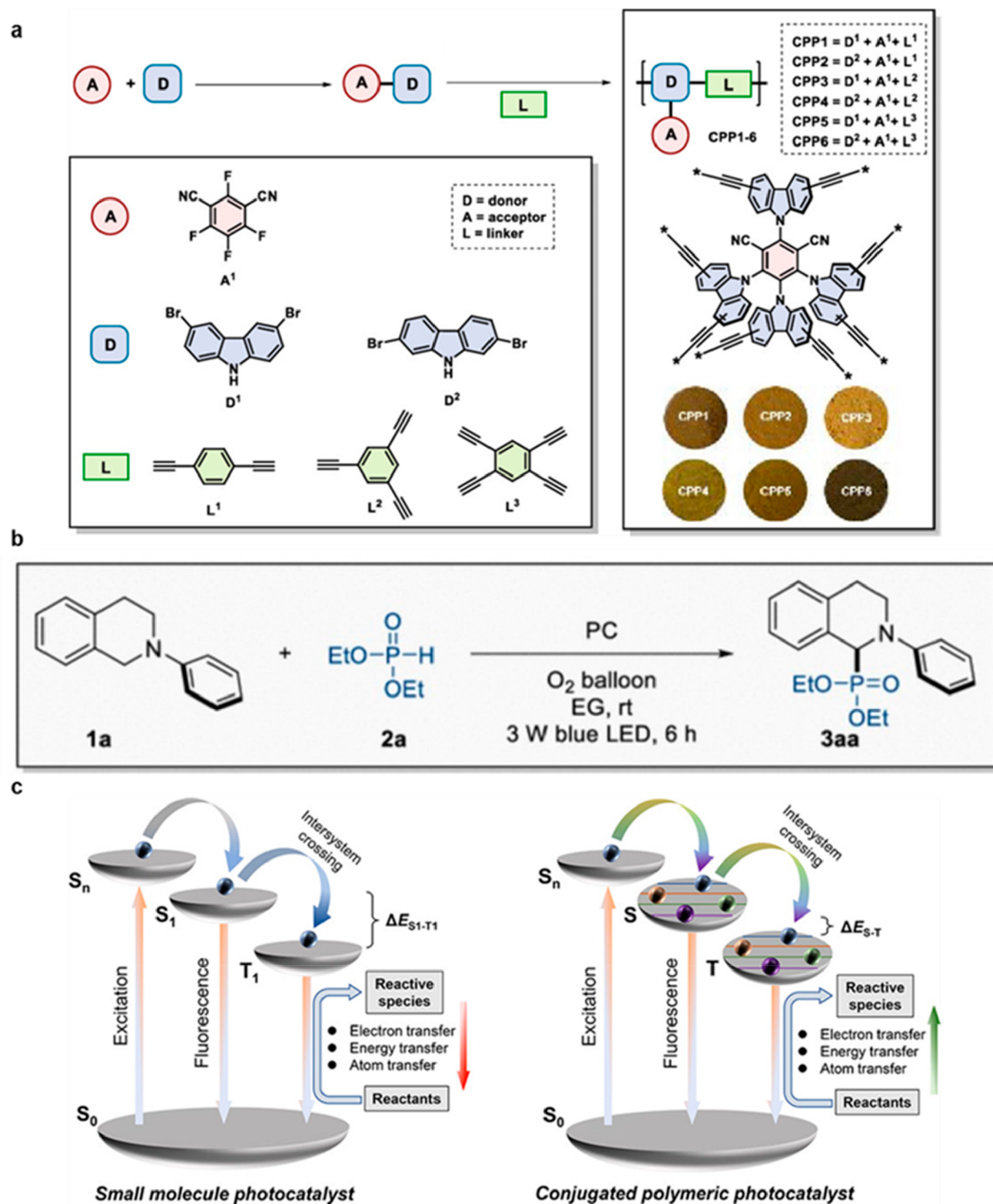
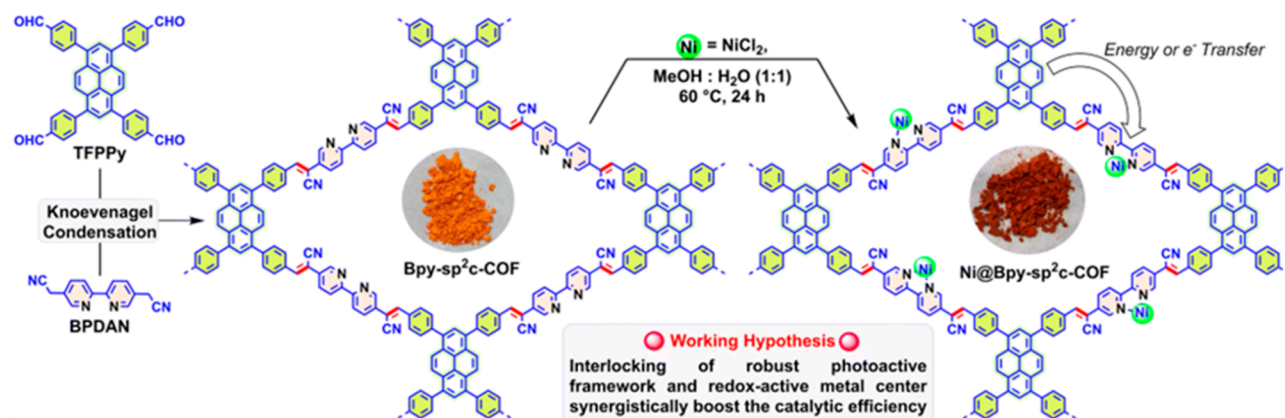


Figure 2. (a) Monomers and synthetic scheme for conjugated polymeric photocatalysts (CPPs) 1–6. (b) Visible light-induced cross dehydrogenative coupling of *N*-phenyltetrahydroisoquinoline (**1a**) with diethyl phosphonate (**2a**). (c) Comparison of photocatalytic process between small molecule and polymer photocatalysts. Adapted with permission from ref 65. Copyright 2022 American Chemical Society.

been synthesized from various photoactive building blocks such as Rose Bengal,^{67,68} BODIPY,⁶⁹ carbazoles,^{65,70} and phenothiazines.⁷¹ For example, Chen, Yu, and co-workers synthesized a series of six CPPs (CPP1–6) based on 1,2,3,5-tetrakis(carbazol-9-yl)-4,6-dicyanobenzene (4CzIPN) monomers via nucleophilic aromatic substitution and Sonogashira–Hagihara coupling (Figure 2a).⁶⁵ These as-synthesized CPPs

were characterized by Fourier-transform infrared (FT-IR) spectroscopy and solid-state cross-polarized magic angle spinning (CP/MAS) ¹³C NMR. Their amorphous nature was confirmed by powder X-ray diffraction (PXRD), and their porosity was assessed by 77 K N₂ sorption measurements, with the CPPs possessing Brunauer–Emmett–Teller (BET) surface areas ranging from 8 to 391 m²/g. In addition, the

a) Catalyst Preparation and Working Hypothesis



b) Diverse C–X (X = B, C, N, O, P, S) Cross-Coupling Reactions

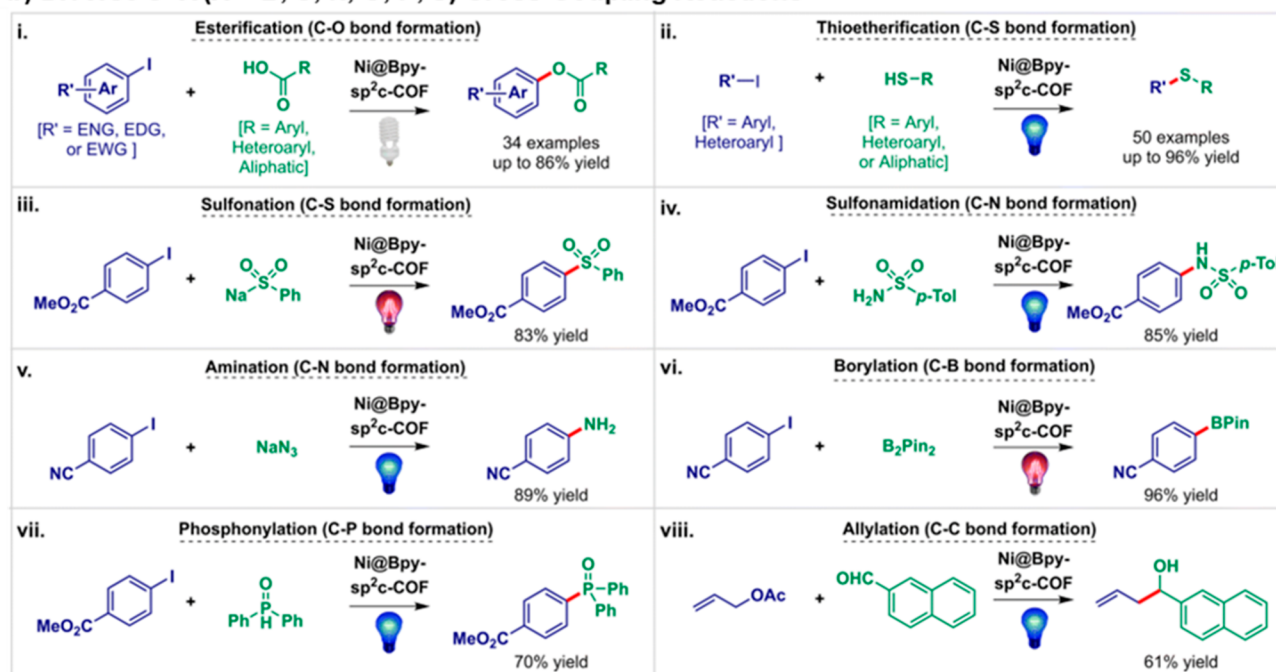


Figure 3. (a) Synthetic scheme for Ni@Bpy-sp²c-COF. (b) Eight visible light-mediated cross-coupling reactions catalyzed by Ni@Bpy-sp²c-COF. Adapted with permission from ref 92. Copyright 2023 Royal Society of Chemistry.

photoabsorption properties of these CPPs were further probed by UV–vis diffuse reflectance spectroscopy (DRS), transient photocurrent response, and electrical impedance spectroscopy (EIS). The latter revealed a smaller radius of the semicircular Nyquist diagram under visible light irradiation than that in the dark, indicating a smaller charge transfer barrier upon photoirradiation. Evaluation of the as-synthesized CPPs as catalysts for the visible light-induced cross-dehydrogenative coupling of *N*-phenyltetrahydroisoquinoline with diethyl phosphonate revealed that all six CPPs were catalytically active, with CPP3 outperforming the other tested materials (Figure 2b). The molecular photocatalyst 4CzIPN was also found to catalyze this reaction, albeit with a much lower yield. The superior photocatalytic performance of CPP3 compared to 4CzIPN was attributed to the enhanced singlet–triplet intersystem crossing (ISC) process resulting from the reduced energy gap between the singlet and triplet excited states after polymerization (Figure 2c). To examine its generality as a heterogeneous photocatalyst, CPP3 was used in a number of

photocatalytic cross-dehydrogenative coupling reactions such as the C1-functionalization of tetrahydroisoquinolines and benzylic and allylic oxygenation reactions. Notably, CPP3, an insoluble polymer, can be recovered from the reaction mixture by centrifugation and directly reused at least four times without an obvious loss in yield. Furthermore, the scanning electron microscopy (SEM) images and IR spectra of CPP3 after recycling match those of freshly prepared CPP3. Beyond C–H functionalization, POPs have also been used to catalyze the photocatalytic oxidative coupling of amines,^{72–75} the aza-Henry reaction,^{76,77} and the reductive dehalogenation of haloketones.^{70,78}

While there are many advantages for using POPs as heterogeneous photocatalysts, such as their ease of synthesis and chemical robustness, they also suffer from several drawbacks. Most POPs have at least partially interpenetrated networks, which not only limits their surface areas but also decreases their pore sizes, thereby hindering substrate diffusion into the pores for efficient catalysis. As a result of their

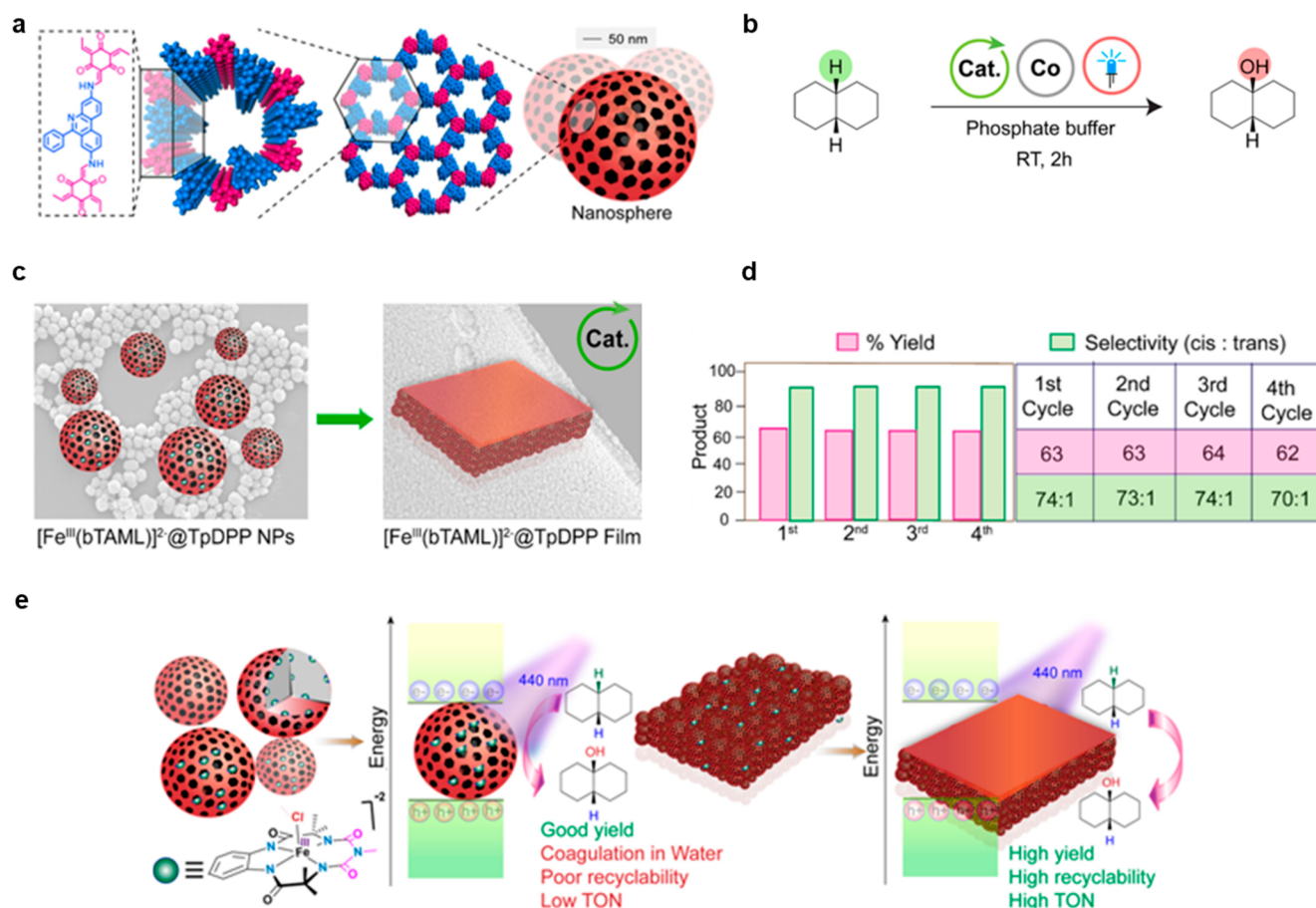


Figure 4. (a) Structure of TpDPP COF. (b) The hydroxylation of *cis*-decalin. (c) The fabrication of $\text{Fe}^{\text{III}}(\text{bTAML})@ \text{TpDPP}$ COF thin film from the corresponding nanospheres. (d) Recycling experiment showing the enhanced recyclability of $\text{Fe}^{\text{III}}(\text{bTAML})@ \text{TpDPP}$ COF thin film. (e) Comparison of the photocatalytic performance of $\text{Fe}^{\text{III}}(\text{bTAML})@ \text{TpDPP}$ COF nanospheres and thin film. Adapted with permission from ref 96. Copyright 2023 American Chemical Society.

amorphous nature and network interpenetration, most POPs do not have uniform pore distributions. Consequently, POPs generally lack well-defined catalytic sites, which complicates efforts to better understand their catalytic behaviors and to rationally design better POPs for heterogeneous photoredox catalysis.⁵⁶

2.2. COFs as Heterogeneous Photocatalysts

COFs, a class of porous and crystalline 2D and 3D polymer networks, have also emerged as a potentially promising platform for heterogeneous photoredox catalysis.³⁴ Because the symmetry, size, and connectivity of the organic building blocks dictate the overall structure of the resulting COFs, the chemical and physical properties of COFs can be rationally tuned by virtue of incorporating different functional building blocks, thereby producing structures with adjustable porosities and functionalities.³⁴ Furthermore, unlike POPs, most COFs possess well-defined and uniform pores, creating a unique local environment that allows for facile substrate diffusion and counterion transport.^{34,56} In addition to their wide study as heterogeneous photocatalysts relevant to energy and the environment,^{61,79–85} COFs have also found application in catalyzing organic transformations such as the selective oxidation of sulfides,^{86,87} C–H borylation,⁸⁸ oxidative hydroxylation,⁸⁹ and various cross-coupling reactions,^{87,90–95} either as pristine materials^{86–89} or as nanohybrids.^{87,90–95} For example, Maji and co-workers synthesized a pyrene-based sp^2

carbon-conjugated COF, Bpy- sp^2c -COF, via the Knoevenagel condensation between 1,3,6,8-tetrakis(4-formylphenyl)pyrene and 5,5'-bis(cyanomethyl)-2,2'-bipyridine (Figure 3a).⁹² The nickel(II) center was postsynthetically installed through the bipyridine moieties to provide the metal-anchored COF, Ni@Bpy- sp^2c -COF, which was shown to catalyze eight visible light-mediated cross-coupling reactions (Figure 3b), with tolerance toward a wide range of coupling partners and yields exceeding those of the homogeneous controls (pyrene + Ni(dtbbpy) Cl_2 , dtbbpy = 4,4'-di-*tert*-butyl-2,2'-bipyridine) and the semi-heterogeneous controls (Bpy- sp^2c -COF + Ni(dtbbpy) Cl_2). In this case, placing the redox-active Ni centers in proximity to the photoactive pyrene-based COF backbone synergistically promotes the catalytic reaction. Notably, the metal-anchored COF also prevents metal leaching and Ni nanoparticle formation, thus enhancing catalyst recyclability and minimizing the risk of product contamination.

As-synthesized COFs have also been employed as metal-free heterogeneous photocatalysts. Recently, Banerjee and co-workers synthesized three different β -keto-enamine-based COFs and assessed their performance for the photocatalytic C–H borylation of nitrogen heterocycles,⁸⁸ which are ubiquitous in drug-like molecules. In most of the reactions tested, TpAzo (formed from 1,3,5-triformylphloroglucinol and 4,4'-azodianiline), the COF with the highest level of crystallinity, highest surface area (2102 m^2/g), broadest visible

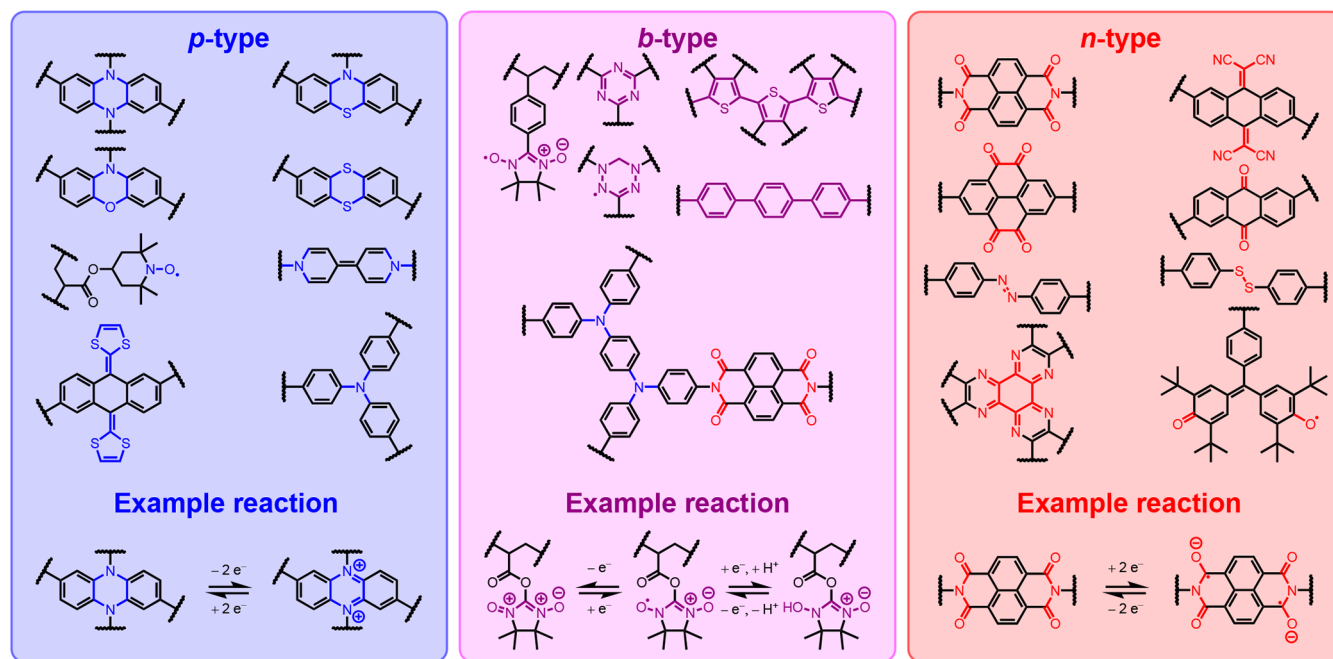


Figure 5. Examples of p-, b-, and n-type redox-active moieties incorporated into polymeric electrodes, and example redox reactions of each type.^{1,21–23,26,111–114}

light absorption (400–750 nm), and lowest band gap (1.89 eV) among the three tested COFs, provides the highest yields. These findings underscore the importance of physical and photophysical parameters such as crystallinity, porosity, light absorbance, and band gap in assessing the photocatalytic performance of organic materials.

Promisingly, confinement of reactive intermediates within COFs has been demonstrated to lead to enhanced catalytic activity and selectivity compared to soluble analogues. For example, Gupta, Banerjee, and co-workers successfully generated and stabilized a catalytically active Fe(IV) species,⁹⁶ namely [(bTAML)Fe^{IV}–O–Fe^{IV}(bTAML)][–] (bTAML = biuret-modified tetraamido macrocyclic ligand) and referred to herein as the Fe₂^{IV}–μ–oxo radical cation, inside the well-defined photoactive nanopores of TpDPP COF (Tp = triformylphloroglucinol; DPP = 3,8-diamino-6-phenylphenanthridine), a phenanthridine-based β-keto-enamine COF (Figure 4a). Following the successful synthesis of colloidal COF nanospheres, the homogeneous (Et₄N)₂[Fe^{III}(Cl)-bTAML] catalyst was postsynthetically immobilized inside the hydrophobic pores of the COF by dispersing the as-synthesized COF nanospheres via sonication. After extensive characterization, the authors propose that, under blue light (440 nm) irradiation, the photoexcited COF oxidizes [Fe^{III}(OH₂)bTAML][–] to the Fe₂^{IV}–μ–oxo radical cation in the presence of aerobic oxygen and [Co^{III}(NH₃)₅Cl]₂, a sacrificial electron acceptor. The proposed intermediate, the Fe₂^{IV}–μ–oxo radical cation, has an electron paramagnetic resonance (EPR) spectrum consistent with a S = 1/2 species and a Mössbauer spectrum resembling an Fe(IV) species. Remarkably, unlike earlier reports of Fe₂^{IV}–μ–oxo species in solution, the pore-confined Fe₂^{IV}–μ–oxo radical cation exhibits high reactivity toward diverse substrates in water, which is attributed to the generation and subsequent stabilization of the oxidized species inside the nanopores of the COF. As a demonstration of their photocatalytic efficacy, the as-synthesized Fe^{III}(bTAML)@TpDPP COF nanospheres

were utilized for the selective oxidation of unactivated C–H bonds. Following extensive optimization, hydroxylation and epoxidation of various alkanes and alkenes were carried out with moderate to good yield and high selectivity. For instance, *cis*-decalin was exclusively hydroxylated at the tertiary carbon with a 50% yield, over 70% stereoretention, turnover number (TON) of 74, and turnover frequency (TOF) of 37 h^{–1} (Figure 4b). However, when the Fe^{III}(bTAML)@TpDPP COF nanospheres were used in a recycling test for the hydroxylation of *cis*-decalin, a considerable decrease in yield (from 50% in the first cycle down to 38% in the third cycle) was observed for subsequent cycles. The mediocre performance of the Fe^{III}(bTAML)@TpDPP COF nanospheres in the recycling test was attributed to catalyst leaching and nanosphere coagulation, which impedes mass transfer to the active sites within the pores of the COF, thereby reducing its catalytic efficacy. To prevent nanosphere agglomeration and to enhance catalytic activity and recyclability, Fe^{III}(bTAML)@TpDPP COF thin film with a thickness of 600 nm was fabricated using covalent self-assembly of Fe^{III}(bTAML)@TpDPP COF nanospheres at the interface of dichloromethane and water (Figure 4c). When the same catalytic transformations outlined above were performed, the Fe^{III}(bTAML)@TpDPP COF thin film was found to exhibit higher activity in terms of yield, regioselectivity, TON, and TOF compared to its nanosphere counterpart (Figure 4e). Gratifyingly, the Fe^{III}(bTAML)@TpDPP COF thin film can be recycled at least four times with no observable loss in yield after the fourth cycle for the hydroxylation of *cis*-decalin (Figure 4d).

The successful deployment of POPs and COFs in heterogeneous photoredox catalysis offers valuable insights into the effects of physical parameters such as crystallinity and porosity on catalytic activity. Recent work by Banerjee and co-workers has demonstrated that the photocatalytic activity of COFs tends to trend with their crystallinity and porosity.⁸⁸ This finding suggests that maximizing long-range order and porosity can enable facile diffusion of substrates to the redox-

active sites within polymers. However, further systematic investigations are required to delineate robust trends among different types of materials. Nevertheless, the redox processes involved in photoredox catalysis and the promise demonstrated by organic materials should inform the development of next-generation heterogeneous redox mediators for electrocatalysis.

3. REDOX PROPERTIES OF ORGANIC ELECTRODE MATERIALS

3.1. Organic Battery Materials

The vast majority of industrial electrochemistry applications, including energy storage and electrocatalysis, employ inorganic materials due to their robustness.^{19,97,98} However, the structural rigidity of inorganic solids generally limits their adaptability toward different charge-compensating ions and solvents and reduces accessible capacities at fast charge/discharge rates. For example, replacing relatively expensive Li in batteries with more abundant alkali metals such as Na and K generally requires specifically tailored strategies such as tandem coupled redox reactions or a redesign of the electrode material to accommodate larger cations.^{99–102} The nature of the counterion can affect the yields of electrochemical reactions,^{103–105} which incentivizes the design of catalytically active materials that are compatible with different electrolytes. Furthermore, the limited porosity and inflexibility of most inorganic solids limits electrocatalysis to highly sensitive surface chemistry.^{106–108} For example, the electrosynthesis of 1-butanol from CO₂ with high Faradaic efficiency (FE) by Bocarsly and co-workers required a precise electrode design of Ni-doped (Cr₂O₃)₃Ga₂O₃,¹⁰⁷ verifying that different means of incorporating Ni into identical (Cr₂O₃)₃Ga₂O₃ samples drastically affects the performance of the resulting electrode materials. Finally, the preparation of inorganic electrodes not only requires intensive extraction and refinement procedures for precious metals such as Co¹⁰⁹ but also high temperatures to convert the precursors into usable electrodes.^{25,110}

Given these limitations, organic electrode materials have garnered increased interest as sustainable materials for electrochemical energy storage (Figure 5).^{1,21–24,26,111–114} Typically, these materials are prepared by incorporating moieties that can be reversibly oxidized and/or reduced into insoluble polymeric backbones (Figure 5). Diverse redox-active functionalities, including but not limited to quinones, phenazines, imides, aminoxyl radicals, and triphenylamines, have been incorporated into polymers for study as battery electrodes.^{22,23,26} Generally, materials are referred to as n-type if they are charge-compensated by cations upon reduction (e.g., quinones), p-type if they are charge compensated by anions upon oxidation (e.g., N-substituted phenazines), and bipolar (b-type) if both phenomena are possible within a single moiety (e.g., verdazyl radicals) or both n- and p-type moieties are present in a single material (Figure 5). Critically, it is not enough to simply incorporate a desired redox-active moiety into a polymer backbone; recent structure–property studies have highlighted the importance of the redox-inactive polymer backbone on the mechanisms of charge compensation and thus battery electrode performance.^{28–31,115–118} Nonetheless, fundamental questions remain about how material properties such as dimensionality, crystallinity, rigidity, and porosity impact the performance of organic electrode materials.²⁶

3.2. Advantages of Organic Electrode Materials

The advantages offered by organic materials over their inorganic counterparts include structural flexibility and tunability, high theoretical gravimetric capacity, and improved sustainability due to the abundant raw materials from which they are derived.^{22,23} The structural flexibility of polymers also allows for reduction/oxidation with multiple charge-compensating ions using a single material, with multiple polymers having demonstrated potential to accommodate Li⁺, Na⁺, and K⁺ within the same polymer matrix,^{28,119–121} which is uncommon for inorganic materials. One notable example is

poly(pentacenetetrone sulfide) (PPTS) examined by Wang and co-workers in Na metal coin cells,¹¹⁷ which achieves a capacity of 160 mAh g⁻¹ at a discharge rate of 10 A g⁻¹ (34.5 C; 1 C is the rate at which the material fully discharges in 1 h).¹¹⁷ The flexibility of organic materials also allows for good capacity retention at fast charge/discharge rates. For example, Abruña, Fors, and co-workers achieved a capacity of 230 mAh g⁻¹ at a discharge rate of 1.0 A g⁻¹ (3.5 C) with the cross-linked phenazine-based polymer poly(Ph-PZ)-10 (poly(N-phenylphenazine) with 10% cross-linking units) in Li metal coin cells,¹²² which retains 86% of its capacity when increasing the discharge rate from 1 to 60 C. These studies credit the high-power capabilities to the large diffusion coefficients for ions through the polymer matrix. Although cycling stability is a persistent challenge for organic electrode materials, several have demonstrated promising cycling stability. For example, Wang, Zhou, and co-workers demonstrated that P14AQ, a polyanthraquinone with a polyphenylene backbone, retains 99.4% of its initial capacity after 1000 charge/discharge cycles.¹²³ The stability of this material is attributed to its high molecular weight, which minimizes dissolution into the electrolyte.

The promising traits for battery materials outlined above are equally appealing for electrocatalysis. A recyclable and stable electroactive material facilitates purification of products and removes the need for frequent catalyst replacement. In addition, adaptability with multiple charge-compensating ions and electrolytes accelerates the optimization of reaction conditions for a desired transformation. The ability to access multiple distinct redox potentials within a single material is beneficial, though not necessary, for electrocatalysis, whereas single output potentials are generally preferred for energy storage; voltage regulators and similarly engineered devices can adapt the output potential to a desired potential to ameliorate this concern. Overall, evaluating insoluble redox-active organic materials as battery electrodes offers insights for their potential utility as electrocatalysts as well.

3.3. Preparation of Organic Electrodes

In this section, we outline common electrochemical techniques used in electrochemical energy storage research and their potential to provide insights for heterogeneous electrosynthesis. Redox-active materials are typically fabricated into electrodes by mixing the active material(s) with a binder and conductive additive (usually a carbon material) into a slurry or suspension before the mixture is deposited onto a current collector (e.g., carbon paper) or conductive electrode material (e.g., glassy carbon). Generally, it is advisable to maximize the amount of active material in the slurry for accurate investigation of the redox properties of the material of interest and high redox-activity; loadings between 40% and 80% active material have been used to understand charge compensation mechanisms and correlate redox behavior with material structure.^{28,30,116,118,122,123} Alternatively, direct synthesis onto a conductive electrode¹²⁴ or electropolymerization¹²⁵ from a functionalized electrode is also possible. However, direct synthesis is more typical of inorganic solids, and electropolymerization has only been demonstrated for a limited range of polymers to date.

Although simple electrodes can be employed directly for electrochemical studies, coin cells enable investigation of a wider range of properties such as long-term stability or cyclability within a device (Figure 6).¹²⁶ Coin cells are sealed differently depending on their architecture, yet they all consist of electrodes (working and counter, and for a three-electrode cell, an additional external independent reference electrode), a separator that prevents direct contact between the working and counter electrode to ensure only ionic conductivity occurs when wetted with electrolyte, spring and spacer to ensure the cell is tightly assembled and that surface contact is guaranteed, and a gasket that ensures the working and counter electrodes are not short-circuited by the case and the cap that enclose and seal the entire system. Two-electrode coin cells are generally preferred due to their simplicity; however, three-electrode coin cells are required for potential-sensitive measurements that necessitate an additional independent reference electrode. In a half-cell, the counter

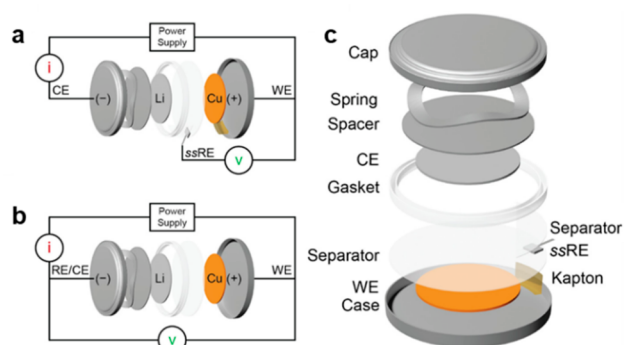


Figure 6. (a) Three-electrode coin cell architecture. (b) Two-electrode coin cell architecture with a Li counter electrode and Cu working electrode. (c) Components of a coin cell. The solid-state reference electrode (ssRE) and Kapton are customized components to transform a two-electrode coin cell into a three-electrode coin cell, and the other components are common to both two- and three-electrode coin cells. Reproduced with permission from ref 126. Copyright 2021 American Chemical Society.

electrode is typically added in excess to singly optimize the working electrode. This is commonly seen in alkali metal batteries such as Li metal coin cells, in which the metal anode is added in significant excess compared to the active material. The materials are then characterized using electrochemical techniques, which are outlined below.

3.4. Solid-State Voltammetry

Voltammetry techniques such as cyclic voltammetry (CV) and linear sweep voltammetry (LSV) are generally used to probe the electrochemical properties of redox-active materials.¹²⁷ CV and LSV are employed to investigate the reversibility, thermodynamics, and kinetics of a given electron transfer event and can be employed similarly for solution- and solid-state systems. One key difference in CV measurements between soluble and insoluble organic compounds is the sweep rate (ν). Solution-state measurements typically are carried out at sweep rates of 10–100 mV/s or higher.^{5,127–129} However, solid-state CVs typically are performed at much slower sweep rates (0.05–1 mV/s) to allow for the diffusion of ions and the conduction of electrons through the material to access the redox-active sites.^{28,130–133} Although fast sweep rates have been used with insoluble polymers,¹²⁸ only qualitative observations such as retention of redox-activity over many CV cycles and changes in behavior with respect to the counterion can typically be examined in this way.

Arguably, the most significant difference between solution- and solid-state electrochemistry is that heterogeneous materials require charge compensation via the significantly slower diffusion of counterions into a solid-state matrix. As a result, solid-state CVs typically show broad peaks and wide peak splitting, necessitating a detailed examination of phenomena such as ion diffusion to understand the redox-activity of insoluble materials. Redox events are often categorized into two behaviors: diffusion-controlled (or diffusion-limited/Faradaic) and surface-controlled (or capacitive/non-Faradaic).¹³⁰ Diffusion-controlled behavior involves redox-activity being limited by the diffusion of solutes toward the electrode, while surface-controlled behavior is characterized by redox-activity being limited by the transfer of charge from the electrode to the substrate. With heterogeneous materials, diffusion limitations originate from ions diffusing or intercalating into the material, while surface-controlled behaviors involve conduction of electrons between the redox-active sites and the current collector. The proportions to which these two behaviors contribute to the overall profile can be determined by carrying out CVs at especially slow sweep rates (0.05–0.1 mV/s) to ensure maximal access to redox-active sites.^{28,115} Occasionally, special features such as uncharacteristically sharp peaks are observed, which indicate a significant structural rearrangement or phase change during charge and/or discharge events.^{28,134}

3.5. Galvanostatic Charge/Discharge Cycling

Galvanostatic charge/discharge (GCD) cycling is a crucial test used in energy storage research to examine the long-term charge capacities and lifetimes of electrode materials. GCD cycling reports on accessible capacity, disparity between charging and discharging processes—determined by the Coulombic efficiency (discharge capacity:charge capacity ratio)—and long-term cycling stability. For example, Zhang and co-workers determined that PI-2, which is composed of a perylene diimide (PDI) core with an ethyl bridging unit from ethylene diamine as the amine linker, demonstrates improved stability compared to related polymers based on naphthalene diimides (NDIs) or pyromellitic diimides (PMDIs) (Figure 7).¹¹⁸ This material stabilizes at 87.5% of its initial capacity

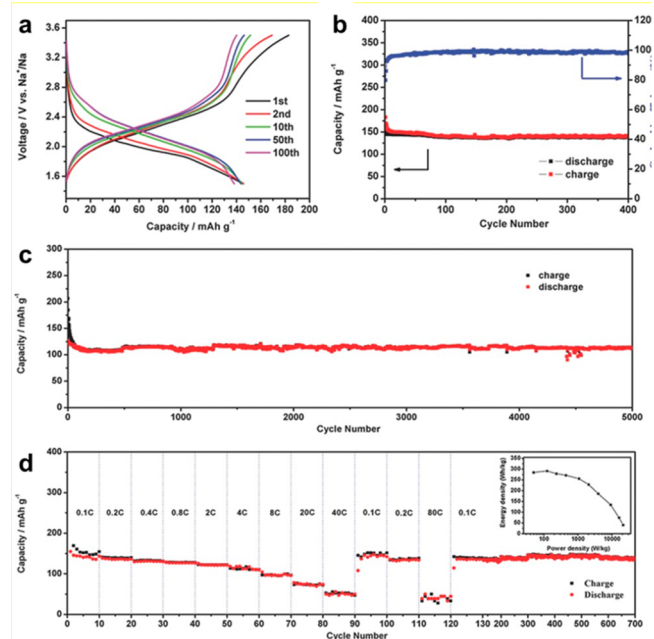


Figure 7. GCD cycling of the PDI polymer PI-2. (a) Individual charge and discharge curves for each cycle. (b) Short-term stability cycling with charge capacity, discharge capacity, and Coulombic efficiency plotted from individual charge/discharge curves. (c) Long-term cycling stability. (d) Rate tests for charge/discharge cycles at different charge/discharge rates between 0.1–80 C. Inset: Ragone plot of PI-2 evaluating the loss of energy density with increased power density. Adapted with permission from ref 118. Copyright 2013 John Wiley and Sons.

over 5000 cycles with Coulombic efficiency close to 100%, demonstrating good reversibility and minimal side processes during charge/discharge. Furthermore, other studies have revealed that a critical factor for attaining long-term materials stability is matching hard–soft acid/base pairs between the polymer material and the charge-compensating ion.^{28,135,136} GCD can also be performed at different charge/discharge rates, and organic materials have especially demonstrated potential as high-power electrodes with reduced capacity losses at fast charge/discharge rates (Figure 7d).^{22,30,117,118} This is often translated as power density vs energy density through a Ragone plot (inset of Figure 7d). In the context of heterogeneous catalysis, high-power densities should help to maximize access to catalytically active species at high currents.

GCD can also be adapted to probe different mechanisms, such as by the addition of crown ethers or replacing the solution-based electrolyte with polymer-based electrolytes. Typically, chelation using crown ethers has been used to suppress dendrite formation.^{137–139} Abruña, Milner, and co-workers tested Li and K half-cells with 12-crown-4 and 18-crown-6 ethers, respectively, to introduce persistent chelating agents and probe ion–electrode interactions within PDI

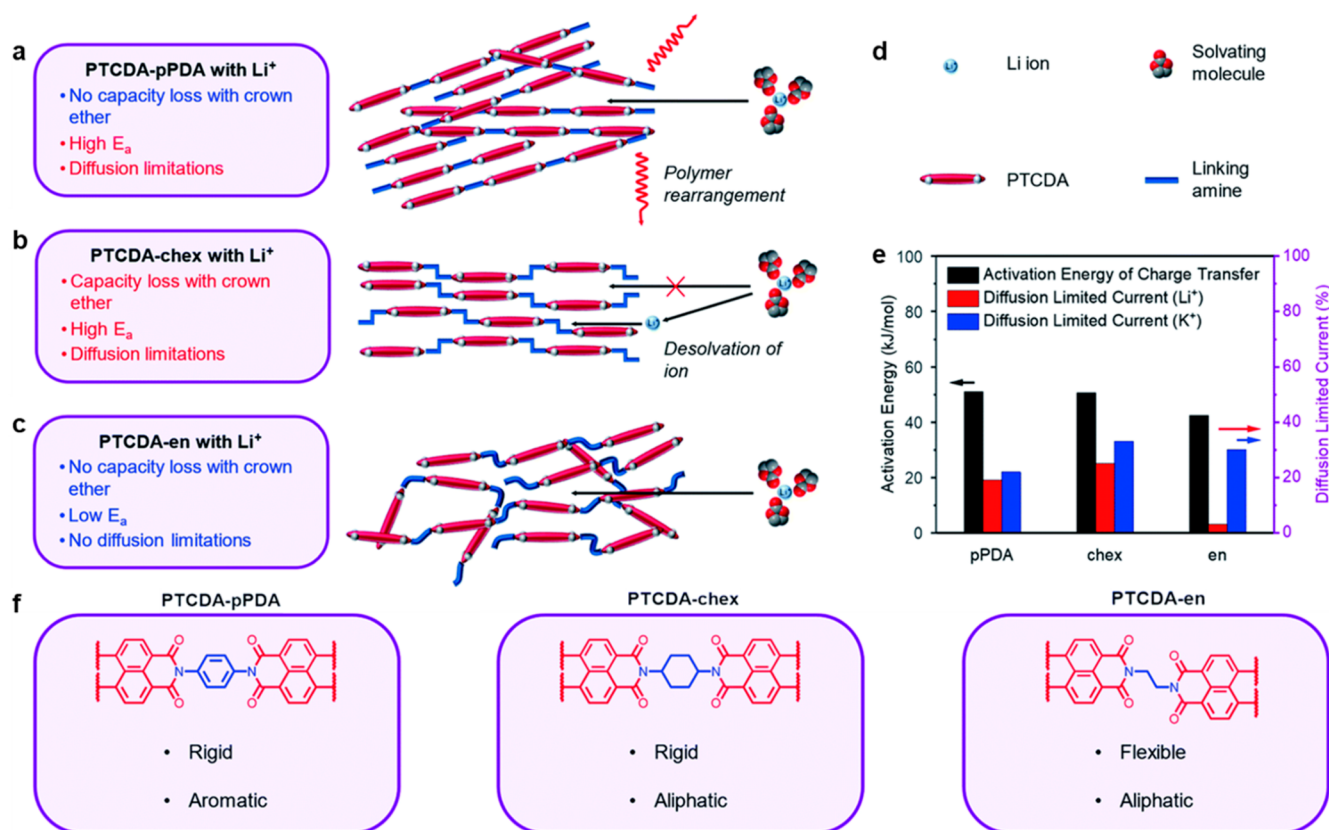


Figure 8. Structural properties of polymers PTCDA-pPDA, PTCDA-chex, and PTCDA-en investigated by Abruña, Milner, and co-workers. (a–d) Proposed charge compensation mechanisms in Li⁺ containing electrolyte solutions based on GCDs. (e) Activation energies of charge transfer with Li⁺ determined by potentiostatic EIS and diffusion-limited current proportion in Li⁺ and K⁺ batteries based on CV tests. (f) Chemical structure and properties of the three polymers. Adapted with permission under a Creative Commons Attribution 3.0 Unported License from ref 28. Copyright 2022 Royal Society of Chemistry.

polymers (Figure 8).²⁸ While the addition of 18-crown-6 to K coin cells drastically decreased performance across all of the tested polymers, the results were mixed for cycling performances in Li coin cells with added 12-crown-4. The authors attribute this to the greater ease of shedding solvent molecules for a softer ion such as K⁺, while Li⁺ has significant solvation even in the absence of a crown ether when entering some of the polymer matrices, depending on the microstructure of the electrode. GCD using ion-conducting polymer-based electrolytes such as poly(ethylene oxide) (PEO) has also been investigated as means to suppress dendrite formation and increase battery lifetimes.^{113,140–142} Alternatively, Troshin and co-workers used polymer electrolytes to hinder the molecular dynamics of electrode materials,³¹ thereby improving their cyclability. They supplemented these results with computational studies to support that the mobility of the electrode polymer strands hindered deintercalation, and thus oxidation, during recharging.

3.6. Electrochemical Techniques for Mechanistic Investigations

Although GCD and CV measurements can provide valuable insight into the redox properties of organic materials, they must be supplemented by other techniques to better probe the mechanisms of charge compensation. For example, galvanostatic intermittent titration technique (GITT)^{117,143} is used to measure diffusion coefficients of charge-compensating ions moving within the electrode material, while EIS^{126,144} is used to determine overall charge transfer activation energies. Electrochemical quartz crystal microbalance with dissipation (EQCM-D) can also be used to sensitively determine the mass changes occurring within a small portion of the electrode during charge and/or discharge and further elucidate ion movements during redox reactions.¹⁴⁴ It is worth noting that many of the organic materials subjected to EQCM-D have been directly electro-

polymerized onto a substrate¹⁴⁵ or dissolved and spin-coated¹⁴⁶ due to the requirement for polymer thin films to carry out these measurements.

Two- or four-point probe conductivity measurements provide electrical conductivity data for organic materials, but the results from these measurements are generally poor indicators for battery performance. For example, Dichtel and co-workers found little correlation between electrical conductivity and cycling performance among four anthraquinone-based COFs ((DAPH-TFP COF, DAAQ-TFP COF, PEDOT@DAPH-TFP COF, and PEDOT@DAAQ-TFP COF; DAPH = 2,6-diaminophenazine, DAAQ = 2,6-diaminoanthroquinone, TFP = 1,3,5-triformylphloroglucinol, PEDOT = poly(3,4-ethylenedioxythiophene)).¹⁴⁷ Instead, they found that the ion diffusion coefficients measured using EIS were more effective predictors for battery performance. In addition, conductivity measurements are typically carried out on materials in their native state and may not accurately reflect the conductivity of the materials after electrochemical charging. Typical slurry compositions also include conductive additives, further obfuscating the utility of such measurements.

Some combination of the outlined electrochemical techniques is generally required to reliably depict the overall mechanisms involved in charging/discharging, which can then be correlated with the physical properties of the materials. For example, Abruña, Milner, and co-workers determined that, within a series of PDI polymers, some amount of flexibility allows for a significant reduction in the polymer charge-transfer barrier (Figure 8).²⁸ In particular, the flexible polymer PTCDA-en (PTCDA = perylene-3,4,9,10-tetracarboxylic dianhydride, en = ethylenediamine) demonstrated a ~9 kJ mol⁻¹ reduction in the kinetic barrier for Li⁺ charging compared to its more rigid counterparts (Figure 8e). However, further increases in polymer

flexibility can hinder ion diffusion by making the polymer more “solvent-like”.^{30,115} This explains why there are conflicting studies regarding the role of backbone flexibility in encouraging fast charge/discharge kinetics in polymer materials.^{29–31,116}

3.7. Spectroelectrochemical Methods

Spectroelectrochemical techniques such as PXRD, X-ray photoelectron spectroscopy (XPS), IR spectroscopy, SEM, transmission electron microscopy (TEM), high-resolution TEM (HR-TEM), Raman spectroscopy, and UV–vis spectroscopy, can complement electrochemical studies to provide insight into how materials change during charge/discharge processes.^{148–150} *Ex situ* investigations are commonly carried out for simplicity due to the need for customized cells and specialized equipment for *in operando* measurements.^{151,152} X-ray techniques such as PXRD^{117,118,153} and electron microscope techniques such as SEM,^{117,154} HR-TEM,¹⁵⁴ and TEM^{117,154} have been used to detect changes in structural morphology over the course of or after GCD cycles. Meanwhile, XPS,^{117,154,155} IR,^{117,153} Raman,¹⁵⁶ SSNMR,¹⁵⁷ and UV–vis^{117,158} spectroscopies have been used to detect changes in functional group environments or verify the recovery of the starting material after GCD cycling. Postmortem electrospray ionization (ESI) mass spectrometry (MS) has been used to interrogate electrode degradation.¹⁵⁸ These techniques all lend insights into the origins of capacity decay and material degradation, which are problematic for both catalysis and energy storage.

With a wide range of techniques available to characterize charge/discharge processes, heterogeneous redox-active organic materials can be thoroughly investigated for their viability for energy storage and/or heterogeneous electrocatalysis. As both applications share many desirable materials properties, such as fast and reversible redox-activity, tunability, cyclability, adaptability to multiple electrolytes, and facile ion diffusion, the potential of a material for both applications can be simultaneously evaluated using the techniques outlined above.

4. ELECTROCATALYSIS USING ORGANIC MATERIALS

In contrast to the wide study of organic materials in the areas of photoredox catalysis (section 2) and energy storage (section 3), organoelectrochemistry using polymer-based redox mediators or electrocatalysts remains significantly understudied. Nonetheless, POPs and COFs have emerged as promising catalysts for environmentally relevant electrocatalytic transformations such as the oxygen reduction reaction (ORR), oxygen evolution reaction (OER), hydrogen evolution reaction (HER), and CO₂ reduction.^{44,46–48} The benefits of these materials over homogeneous electrocatalysis include colocalization of active sites, stabilization of reactive species, and recyclability. In this section, we further elaborate the advantages of POPs and COFs as heterogeneous mediators for electrocatalysis, with the goal of highlighting their potential future utility for electrosynthesis.

Although a variety of catalysts are suitable for CO₂ reduction, traditional monometallic catalysts tend to have high overpotentials, poor selectivity, and susceptibility to competitive HER.^{159–162} To improve the selectivity and efficiency of CO₂ reduction, two strategies have been employed: exposing specific crystal lattice planes on electrodes and incorporating catalytic sites into metal complexes and polymers.^{163,164} Compared to higher density materials, POPs and COFs stand out because they provide ready access to catalyst sites due to their highly porous structures. As such, catalytically active metals such as Fe, Co, Ni, Cu, Mn, and Re can be easily incorporated into POPs or COFs and employed for CO₂ reduction.^{165,166} Redox-active polymers such as COF-300, COF-366, COF-367, and pyrimidine-containing POPs (PyPOPs) have been explored as catalyst supports or cocatalysts for the electrochemical reduction of CO₂ to CO,⁴⁴ which involves multiple electron–proton transfers between CO₂ molecules and redox-active polymers on the electrode surface.¹⁵

4.1. Colocalization of Active Sites

Beyond simple immobilization of catalytically active species, COFs offer the unique opportunity to colocalize functional groups to achieve synergistic catalysis, similar to the examples outlined above in

the context of photoredox catalysis (Figure 3). For example, Deng and co-workers designed a molecular interface by combining the catalytic surface of a Ag electrode with COF-300-AR (AR = “after reduction”), a secondary amine-functionalized COF (Figure 9).¹⁶⁷ The authors

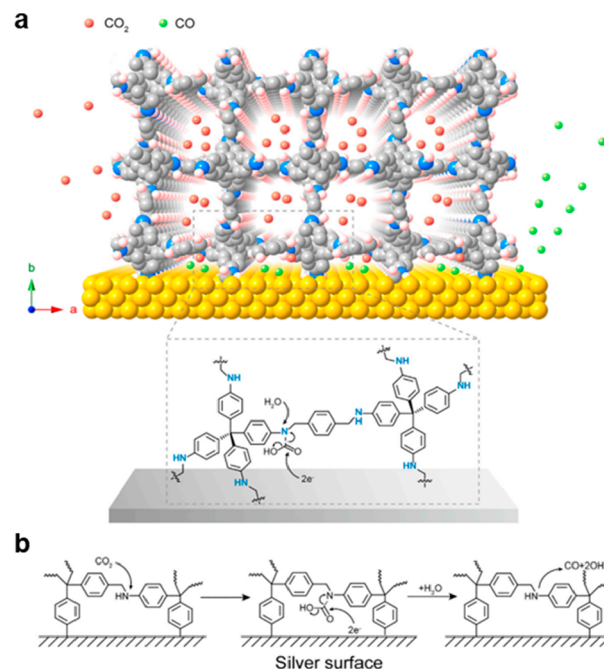


Figure 9. (a) Molecular interface of COF-300-AR with Ag electrode surface. (b) Mechanism of concerted CO₂ reduction at the interface between the COF and the Ag electrode via carbamate formation. Reproduced with permission from ref 167. Copyright 2018 Elsevier Inc.

demonstrate that CO₂ molecules are converted to carbamates within the COF by CP/MAS ¹³C SSNMR. They propose that the generated carbamates are then reduced at the Ag surface (Figure 9b). Subsequently, CO molecules and OH⁻ anions are released from the material, and the amine functional groups in the COF are regenerated to close the catalytic cycle. The COF plays a critical role in reducing the HER side reaction compared to the native Ag electrode, as demonstrated by the suppression of HER from 80% to 22% and an increase of CO FE from 13% to 53% at −0.70 V vs regular hydrogen electrode (RHE). Similar HER suppression has been reported with other types of COF-electrode composites,^{164,168} demonstrating the generality of this colocalization strategy. The ability to colocalize substrates and catalytic species distinguishes COFs from traditional heterogeneous electrocatalysts.

4.2. Immobilization of Catalytic Moieties

Catalytically active species can be immobilized on electrode surfaces or within COFs, POPs, and related metal–organic frameworks (MOFs) to prevent common deactivation pathways in solution such as self-association and unproductive reaction at the counter electrode. For example, 2,2,6,6-tetramethylpiperidine N-oxyl (TEMPO) is the archetypal homogeneous catalyst for the electrochemical oxidation of alcohols to aldehydes and ketones.^{169,170} However, its catalytic efficiency is limited by its slow diffusion to the electrode surface and by dimerization in solution.¹⁷¹ To overcome these limitations, Das and Stahl synthesized a pyrene–TEMPO conjugate, which they immobilized onto glassy carbon (GC) or carbon cloth (CC)-multiwalled carbon nanotube (MWCNT) electrodes by dipping them into an acetonitrile solution of the conjugate (Figure 10a).¹⁷² Remarkably, the surface-immobilized pyrene–TEMPO conjugate was able to effectively catalyze the oxidation of benzyl alcohol to benzaldehyde at low catalyst loadings (0.05 mol %), whereas 4-acetamido-TEMPO, a soluble TEMPO-based catalyst, provided

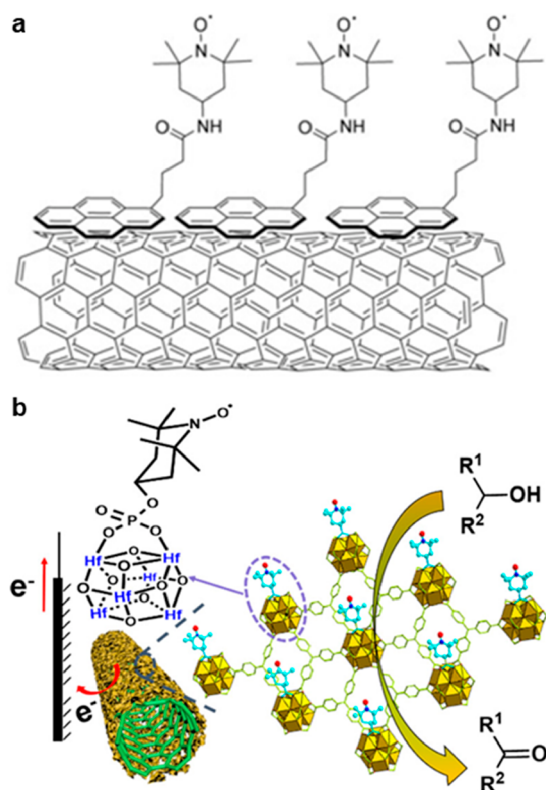


Figure 10. (a) Surface immobilization of pyrene–TEMPO conjugate on MWCNTs. Adapted with permission from ref 172. Copyright 2017 John Wiley and Sons. (b) MOL immobilized on MWCNTs. Reproduced with permission from ref 174. Copyright 2018 American Chemical Society.

negligible conversion of benzyl alcohol under the same conditions. Likewise, Minter and co-workers immobilized 4-glycidyl-TEMPO onto a linear poly(ethylenimine) (LPEI) backbone,¹⁷³ which was then cross-linked onto the surface of a glassy carbon electrode to form a hydrogel through which substrates could easily diffuse. The resulting immobilized catalyst was able to catalyze alcohol oxidation more efficiently than the homogeneous analogue.

Wang and co-workers constructed two TEMPO-based composites with Hf-based metal–organic layers (MOLs) on conductive MWCNTs by replacing some of the formates on the MOL secondary building units with TEMPO-CO₂H free radical and TEMPO-OPO₃H₂ (Figure 10b).¹⁷⁴ The resulting materials, CNT/MOL-TEMPO-CO₂⁻ and CNT/MOL-TEMPO-OPO₃²⁻, possess superior catalytic performances compared to a homogeneous solution of TEMPO in the oxidation of benzyl alcohol to benzaldehyde at low catalyst loadings (0.02 mol %). CNT/MOL-TEMPO-CO₂⁻ and CNT/MOL-TEMPO-OPO₃²⁻ also have a higher FE (97%) for alcohol oxidation compared to the homogeneous TEMPO solution (62%). The authors propose that the decrease in FE for the homogeneous system is due to TEMPO[•] being reduced at the counter electrode, which is prevented when TEMPO is immobilized in the MOL. Furthermore, because of the proposed strong phosphate-MOL binding, CNT/MOL-TEMPO-OPO₃²⁻ could be reused six times without significant loss of activity. Thus, immobilization offers multiple advantages such as recyclability and reduced catalyst degradation.

The examples provided herein demonstrate that redox-active organic and metal–organic materials possess enhanced reactivity compared to their homogeneous analogues in some cases. However, their potential to address challenges in organic synthesis remains largely untapped, with alcohol oxidation being the only synthetic transformation that has been widely studied to date.

5. CONCLUSION

The incorporation of redox-active moieties within (porous) organic materials enables the molecular-level design of heterogeneous catalysts and battery materials. In terms of catalysis, electroactive polymers offer numerous advantages compared to their homogeneous counterparts, including recyclability, robustness, and the ability to engineer various material properties (e.g., porosity, flexibility) through rational structural design. Additionally, immobilization of reactive species that would otherwise decompose in solution and colocalization of incompatible functional groups provide additional opportunities to expand the scope of motifs that can be utilized for redox catalysis. As a result, POPs and COFs are already widely used for photoredox catalysis, and their utility for electrochemical transformations such as alcohol oxidation has been validated.

Despite the advantages outlined above, the opportunity to utilize redox-active polymers as next-generation heterogeneous electrocatalysts and redox mediators relevant to organic synthesis remains underexplored. We propose that multiple hurdles must be overcome to further the development of heterogeneous organic redox mediators. First, from an engineering perspective, there is an unmet need to fabricate organic electrode materials on large scale. Currently, there are no commercially available functionalized organic electrodes, and in the battery community, polymers are generally prepared and processed into electrodes from scratch. Thus, strategies to produce functionalized electrodes and make them compatible with commercial electrolysis set-ups are needed. Further, chemical rationale is required to strategically incorporate redox-active moieties into polymer backbones in order to balance electron/hole conductivity, ion diffusion, and substrate access to catalytically active sites, whereas electrochemical characterization requires distinct expertise. Thus, the field of heterogeneous organoelectrocatalysis requires close collaboration between the polymer science, organic chemistry, and electrochemistry communities to address challenges associated with the design, characterization, and large-scale production of heterogeneous organic electrode materials.

Moving forward, further efforts are needed to unlock novel reactivity patterns in the solid state using redox-active organic materials. Studies in energy storage and photocatalysis have produced systematic guidelines to achieve desired material properties and catalytic outcomes. Based on the work outlined above, imparting flexibility or porosity into polymer materials will likely facilitate catalysis through facile substrate diffusion, while adjusting ion–polymer interactions will enable balance of polymer stability and electrocatalytic activity. We envision that interdisciplinary efforts will unlock the full potential of redox-active materials as sustainable catalysts for the synthesis of complex molecules.

AUTHOR INFORMATION

Corresponding Author

Phillip J. Milner – Department of Chemistry and Chemical Biology, Cornell University, Ithaca, New York 14853, United States; orcid.org/0000-0002-2618-013X; Email: pjm347@cornell.edu

Authors

Jaehwan Kim – Department of Chemistry and Chemical Biology, Cornell University, Ithaca, New York 14853, United States; orcid.org/0000-0003-1311-4982

Jianheng Ling – Department of Chemistry and Chemical Biology, Cornell University, Ithaca, New York 14853, United States; orcid.org/0000-0002-9821-2188

Yihuan Lai – Department of Chemistry and Chemical Biology, Cornell University, Ithaca, New York 14853, United States

Complete contact information is available at:

<https://pubs.acs.org/10.1021/acsmaterialsau.3c00096>

Author Contributions

CRedit: **Jaehwan Kim** conceptualization, writing-original draft, writing-review & editing; **Jianheng Ling** conceptualization, writing-original draft, writing-review & editing; **Yihuan Lai** conceptualization, writing-original draft, writing-review & editing; **Phillip J Milner** conceptualization, writing-original draft, writing-review & editing.

Funding

The development of redox mediators relevant to organic synthesis was supported by the National Institute of General Medical Sciences of the National Institutes of Health under award number R35GM138165 (J.K., Y.L., P.J.M.). The content is solely the responsibility of the authors and does not necessarily represent the official views of the National Institutes of Health. The development of reducing heterogeneous electrophotocatalysts is supported by the U.S. Department of Energy, Office of Science, Office of Basic Energy Sciences under award number DE-SC0024199 (J.L., P.J.M.). We acknowledge the support of a Camille Dreyfus Teacher-Scholar Award to P.J.M. (TC-23-048).

Notes

The authors declare no competing financial interest.

REFERENCES

- (1) Shea, J. J.; Luo, C. Organic Electrode Materials for Metal Ion Batteries. *ACS Appl. Mater. Interfaces* **2020**, *12* (5), 5361–5380.
- (2) Ramachandran, R.; Chen, T.-W.; Chen, S.-M.; Baskar, T.; Kannan, R.; Elumalai, P.; Raja, P.; Jeyapragasam, T.; Dinakaran, K.; Gnana Kumar, G. P. A Review of the Advanced Developments of Electrochemical Sensors for the Detection of Toxic and Bioactive Molecules. *Inorg. Chem. Front.* **2019**, *6* (12), 3418–3439.
- (3) Ribeiro, R. P. P. L.; Grande, C. A.; Rodrigues, A. E. Electric Swing Adsorption for Gas Separation and Purification: A Review. *Sep. Sci. Technol.* **2014**, *49* (13), 1985–2002.
- (4) Botte, G. G. Electrochemical Manufacturing in the Chemical Industry. *Electrochem. Soc. Interface* **2014**, *23* (3), 49–55.
- (5) Novaes, L. F. T.; Liu, J.; Shen, Y.; Lu, L.; Meinhardt, J. M.; Lin, S. Electrocatalysis as an Enabling Technology for Organic Synthesis. *Chem. Soc. Rev.* **2021**, *50* (14), 7941–8002.
- (6) Zhu, C.; Ang, N. W. J.; Meyer, T. H.; Qiu, Y.; Ackermann, L. Organic Electrochemistry: Molecular Syntheses with Potential. *ACS Cent. Sci.* **2021**, *7* (3), 415–431.
- (7) Wiebe, A.; Gieshoff, T.; Möhle, S.; Rodrigo, E.; Zirbes, M.; Waldvogel, S. R. Electrifying Organic Synthesis. *Angew. Chem., Int. Ed.* **2018**, *57* (20), 5594–5619.
- (8) Yan, M.; Kawamata, Y.; Baran, P. S. Synthetic Organic Electrochemical Methods since 2000: On the Verge of a Renaissance. *Chem. Rev.* **2017**, *117* (21), 13230–13319.
- (9) Horn, E. J.; Rosen, B. R.; Baran, P. S. Synthetic Organic Electrochemistry: An Enabling and Innately Sustainable Method. *ACS Cent. Sci.* **2016**, *2*, 302.
- (10) Cardoso, D. S. P.; Šljukić, B.; Santos, D. M. F.; Sequeira, C. A. C. Organic Electrosynthesis: From Laboratory Practice to Industrial Applications. *Org. Process Res. Dev.* **2017**, *21* (9), 1213–1226.
- (11) Liu, J.; Lu, L.; Wood, D.; Lin, S. New Redox Strategies in Organic Synthesis by Means of Electrochemistry and Photochemistry. *ACS Cent. Sci.* **2020**, *6* (8), 1317–1340.
- (12) Smith, J. M.; Harwood, S. J.; Baran, P. S. Radical Retrosynthesis. *Acc. Chem. Res.* **2018**, *51* (8), 1807–1817.
- (13) Steckhan, E. Indirect Electroorganic Syntheses—A Modern Chapter of Organic Electrochemistry [New Synthetic Methods(59)]. *Angew. Chem., Int. Ed. Engl.* **1986**, *25* (8), 683–701.
- (14) Lai, Y.; Halder, A.; Kim, J.; Hicks, T. J.; Milner, P. J. Electroreductive Radical Borylation of Unactivated (Hetero)Aryl Chlorides Without Light by Using Cumulene-Based Redox Mediators. *Angew. Chem., Int. Ed.* **2023**, *62*, No. e202310246.
- (15) Zhu, D. D.; Liu, J. L.; Qiao, S. Z. Recent Advances in Inorganic Heterogeneous Electrocatalysts for Reduction of Carbon Dioxide. *Adv. Mater.* **2016**, *28* (18), 3423–3452.
- (16) Francke, R.; Little, R. D. Redox Catalysis in Organic Electrosynthesis: Basic Principles and Recent Developments. *Chem. Soc. Rev.* **2014**, *43* (8), 2492.
- (17) Jackson, M. N.; Surendranath, Y. Molecular Control of Heterogeneous Electrocatalysis through Graphite Conjugation. *Acc. Chem. Res.* **2019**, *52* (12), 3432–3441.
- (18) Bullock, R. M.; Das, A. K.; Appel, A. M. Surface Immobilization of Molecular Electrocatalysts for Energy Conversion. *Chem.-Eur. J.* **2017**, *23* (32), 7626–7641.
- (19) Dunn, B.; Kamath, H.; Tarascon, J.-M. Electrical Energy Storage for the Grid: A Battery of Choices. *Science* **2011**, *334* (6058), 928–935.
- (20) Fan, E.; Li, L.; Wang, Z.; Lin, J.; Huang, Y.; Yao, Y.; Chen, R.; Wu, F. Sustainable Recycling Technology for Li-Ion Batteries and Beyond: Challenges and Future Prospects. *Chem. Rev.* **2020**, *120* (14), 7020–7063.
- (21) Shi, R.; Jiao, S.; Yue, Q.; Gu, G.; Zhang, K.; Zhao, Y. Challenges and Advances of Organic Electrode Materials for Sustainable Secondary Batteries. *Exploration* **2022**, *2* (4), No. 20220066.
- (22) Gannett, C. N.; Melecio-Zambrano, L.; Theibault, M. J.; Peterson, B. M.; Fors, B. P.; Abruña, H. D. Organic Electrode Materials for Fast-Rate, High-Power Battery Applications. *Materials Reports: Energy* **2021**, *1* (1), No. 100008.
- (23) Esser, B.; Dolhem, F.; Becuwe, M.; Poizot, P.; Vlad, A.; Brandell, D. A Perspective on Organic Electrode Materials and Technologies for next Generation Batteries. *J. Power Sources* **2021**, *482*, No. 228814.
- (24) Muench, S.; Wild, A.; Friebe, C.; Häupler, B.; Janoschka, T.; Schubert, U. S. Polymer-Based Organic Batteries. *Chem. Rev.* **2016**, *116* (16), 9438–9484.
- (25) Larcher, D.; Tarascon, J. M. Towards Greener and More Sustainable Batteries for Electrical Energy Storage. *Nat. Chem.* **2015**, *7* (1), 19–29.
- (26) Banerjee, A.; Khossossi, N.; Luo, W.; Ahuja, R. Promise and Reality of Organic Electrodes from Materials Design and Charge Storage Perspective. *J. Mater. Chem. A* **2022**, *10* (29), 15215–15234.
- (27) Kim, J.; Kim, Y.; Yoo, J.; Kwon, G.; Ko, Y.; Kang, K. Organic Batteries for a Greener Rechargeable World. *Nat. Rev. Mater.* **2023**, *8* (1), 54–70.
- (28) Gannett, C. N.; Kim, J.; Tirtariyadi, D.; Abruña, H. D.; Milner, P. J. Investigation of Ion-Electrode Interactions of Linear Polyimides and Alkali Metal Ions for Next Generation Alternative-Ion Batteries. *Chem. Sci.* **2022**, *13*, 9191.
- (29) Grignon, E.; Battaglia, A. M.; Liu, J. T.; McAllister, B. T.; Seferos, D. S. Influence of Backbone on the Performance of Pendant Polymer Electrode Materials in Li-Ion Batteries. *ACS Appl. Mater. Interfaces* **2023**, *15* (38), 45345–45353.
- (30) Tong, Z.; Tian, S.; Wang, H.; Shen, D.; Yang, R.; Lee, C. S. Tailored Redox Kinetics, Electronic Structures and Electrode/

Electrolyte Interfaces for Fast and High Energy-Density Potassium-Organic Battery. *Adv. Funct. Mater.* **2020**, *30* (5), No. 1907656.

(31) Shestakov, A. F.; Romanyuk, O. E.; Mumyatov, A. V.; Luchkin, S. Y.; Slesarenko, A. A.; Yarmolenko, O. V.; Stevenson, K. J.; Troshin, P. A. Theoretical and Experimental Evidence for Irreversible Lithiation of the Conformationally Flexible Polyimide: Impact on Battery Performance. *J. Electroanal. Chem.* **2019**, *836*, 143–148.

(32) Gong, Y.-N.; Guan, X.; Jiang, H.-L. Covalent Organic Frameworks for Photocatalysis: Synthesis, Structural Features, Fundamentals and Performance. *Coord. Chem. Rev.* **2023**, *475*, No. 214889.

(33) López-Magano, A.; Daliran, S.; Oveisi, A. R.; Mas-Ballesté, R.; Dhakshinamoorthy, A.; Alemán, J.; García, H.; Luque, R. Recent Advances in the Use of Covalent Organic Frameworks as Heterogeneous Photocatalysts in Organic Synthesis. *Adv. Mater.* **2023**, *35* (24), No. 2209475.

(34) Chen, H.; Jena, H. S.; Feng, X.; Leus, K.; Van Der Voort, P. Engineering Covalent Organic Frameworks as Heterogeneous Photocatalysts for Organic Transformations. *Angew. Chem., Int. Ed.* **2022**, *61* (47), No. e202204938.

(35) Bi, S. Photoredox Catalysis by Covalent Organic Frameworks. In *Covalent Organic Frameworks*; IntechOpen, 2022. DOI: 10.5772/intechopen.107485.

(36) Ferguson, C. T. J.; Zhang, K. A. I. Classical Polymers as Highly Tunable and Designable Heterogeneous Photocatalysts. *ACS Catal.* **2021**, *11* (15), 9547–9560.

(37) You, J.; Zhao, Y.; Wang, L.; Bao, W. Recent Developments in the Photocatalytic Applications of Covalent Organic Frameworks: A Review. *J. Clean. Prod.* **2021**, *291*, No. 125822.

(38) Dai, C.; Liu, B. Conjugated Polymers for Visible-Light-Driven Photocatalysis. *Energy Environ. Sci.* **2020**, *13* (1), 24–52.

(39) Zhang, T.; Xing, G.; Chen, W.; Chen, L. Porous Organic Polymers: A Promising Platform for Efficient Photocatalysis. *Mater. Chem. Front.* **2020**, *4* (2), 332–353.

(40) Xu, Z.-Y.; Luo, Y.; Wang, H.; Zhang, D.-W.; Li, Z.-T. Porous Organic Polymers as Heterogeneous Catalysts for Visible Light-Induced Organic Transformations. *Chin. J. Org. Chem.* **2020**, *40* (11), 3777.

(41) Wang, G.-B.; Li, S.; Yan, C.-X.; Zhu, F.-C.; Lin, Q.-Q.; Xie, K.-H.; Geng, Y.; Dong, Y.-B. Covalent Organic Frameworks: Emerging High-Performance Platforms for Efficient Photocatalytic Applications. *J. Mater. Chem. A* **2020**, *8* (15), 6957–6983.

(42) Lei, H.; Zhang, Q.; Liang, Z.; Guo, H.; Wang, Y.; Lv, H.; Li, X.; Zhang, W.; Apfel, U.; Cao, R. Metal-Corrole-Based Porous Organic Polymers for Electrochemical Oxygen Reduction and Evolution Reactions. *Angew. Chem., Int. Ed.* **2022**, *61* (24), No. e202201104.

(43) Nayak, B.; Mukherjee, A.; Basu, S.; Bhanja, P.; Jena, B. K. Metal-Free Triazine-Based Porous Organic Polymer-Derived N-Doped Porous Carbons as Effective Electrocatalysts for Oxygen Reduction Reaction. *ACS Appl. Energy Mater.* **2022**, *5* (12), 15899–15908.

(44) Yang, D.-H.; Tao, Y.; Ding, X.; Han, B.-H. Porous Organic Polymers for Electrocatalysis. *Chem. Soc. Rev.* **2022**, *51* (2), 761–791.

(45) Zhao, X.; Pachfule, P.; Li, S.; Langenhahn, T.; Ye, M.; Schlesiger, C.; Praetz, S.; Schmidt, J.; Thomas, A. Macro/Microporous Covalent Organic Frameworks for Efficient Electrocatalysis. *J. Am. Chem. Soc.* **2019**, *141* (16), 6623–6630.

(46) Fan, Y.; Chen, M.; Xu, N.; Wang, K.; Gao, Q.; Liang, J.; Liu, Y. Recent Progress on Covalent Organic Framework Materials as CO₂ Reduction Electrocatalysts. *Front. Chem.* **2022**, *10*, No. 942492.

(47) Ma, L.; Gao, X.; Liu, X.; Gu, X.; Li, B.; Mao, B.; Sun, Z.; Gao, W.; Jia, X.; Chen, J. Recent Advances in Organic Electrosynthesis Using Heterogeneous Catalysts Modified Electrodes. *Chin. Chem. Lett.* **2023**, *34* (4), No. 107735.

(48) Ali, T.; Wang, H.; Iqbal, W.; Bashir, T.; Shah, R.; Hu, Y. Electro-Synthesis of Organic Compounds with Heterogeneous Catalysis. *Adv. Sci.* **2023**, *10* (1), No. 2205077.

(49) Alsudairy, Z.; Brown, N.; Campbell, A.; Ambus, A.; Brown, B.; Smith-Petty, K.; Li, X. Covalent Organic Frameworks in Heteroge-

neous Catalysis: Recent Advances and Future Perspective. *Mater. Chem. Front.* **2023**, *7* (16), 3298–3331.

(50) Cheng, H.; Wang, T. Covalent Organic Frameworks in Catalytic Organic Synthesis. *Adv. Synth. Catal.* **2021**, *363* (1), 144–193.

(51) Debruyne, M.; Van Speybroeck, V.; Van Der Voort, P.; Stevens, C. V. Porous Organic Polymers as Metal Free Heterogeneous Organocatalysts. *Green Chem.* **2021**, *23* (19), 7361–7434.

(52) Yusran, Y.; Li, H.; Guan, X.; Fang, Q.; Qiu, S. Covalent Organic Frameworks for Catalysis. *EnergyChem.* **2020**, *2* (3), No. 100035.

(53) Guo, J.; Jiang, D. Covalent Organic Frameworks for Heterogeneous Catalysis: Principle, Current Status, and Challenges. *ACS Cent. Sci.* **2020**, *6* (6), 869–879.

(54) Enjamuri, N.; Sarkar, S.; Reddy, B. M.; Mondal, J. Design and Catalytic Application of Functional Porous Organic Polymers: Opportunities and Challenges. *Chem. Rec.* **2019**, *19* (9), 1782–1792.

(55) Zhang, Y.; Riduan, S. N. Functional Porous Organic Polymers for Heterogeneous Catalysis. *Chem. Soc. Rev.* **2012**, *41* (6), 2083–2094.

(56) Kaur, P.; Hupp, J. T.; Nguyen, S. T. Porous Organic Polymers in Catalysis: Opportunities and Challenges. *ACS Catal.* **2011**, *1* (7), 819–835.

(57) Shaw, M. H.; Twilton, J.; MacMillan, D. W. C. Photoredox Catalysis in Organic Chemistry. *J. Org. Chem.* **2016**, *81* (16), 6898–6926.

(58) Mathur, S.; Rogers, B.; Wei, W. Organic Conjugated Polymers and Polymer Dots as Photocatalysts for Hydrogen Production. *Front. Energy* **2021**, *15* (3), 667–677.

(59) Banerjee, T.; Podjaski, F.; Kröger, J.; Biswal, B. P.; Lotsch, B. V. Polymer Photocatalysts for Solar-to-Chemical Energy Conversion. *Nat. Rev. Mater.* **2021**, *6* (2), 168–190.

(60) Xu, C.; Zhang, W.; Tang, J.; Pan, C.; Yu, G. Porous Organic Polymers: An Emerged Platform for Photocatalytic Water Splitting. *Front. Chem.* **2018**, *6*, 592.

(61) Li, Y.; Song, X.; Zhang, G.; Wang, L.; Liu, Y.; Chen, W.; Chen, L. 2D Covalent Organic Frameworks Toward Efficient Photocatalytic Hydrogen Evolution. *ChemSusChem* **2022**, *15* (15), No. 00901, DOI: 10.1002/cssc.202200901.

(62) Li, X.; Kawai, K.; Fujitsuka, M.; Osakada, Y. COF-Based Photocatalyst for Energy and Environment Applications. *Surf. Interfaces* **2021**, *25*, No. 101249.

(63) Wang, H.; Wang, H.; Wang, Z.; Tang, L.; Zeng, G.; Xu, P.; Chen, M.; Xiong, T.; Zhou, C.; Li, X.; Huang, D.; Zhu, Y.; Wang, Z.; Tang, J. Covalent Organic Framework Photocatalysts: Structures and Applications. *Chem. Soc. Rev.* **2020**, *49* (12), 4135–4165.

(64) He, Z.; Goulas, J.; Parker, E.; Sun, Y.; Zhou, X.; Fei, L. Review on Covalent Organic Frameworks and Derivatives for Electrochemical and Photocatalytic CO₂ Reduction. *Catal. Today* **2023**, *409*, 103–118.

(65) Zhu, S.-S.; Liu, Y.; Chen, X.-L.; Qu, L.-B.; Yu, B. Polymerization-Enhanced Photocatalysis for the Functionalization of C(sp³)-H Bonds. *ACS Catal.* **2022**, *12* (1), 126–134.

(66) Xie, Z.; Wang, C.; deKrafft, K. E.; Lin, W. Highly Stable and Porous Cross-Linked Polymers for Efficient Photocatalysis. *J. Am. Chem. Soc.* **2011**, *133* (7), 2056–2059.

(67) Yu, X.; Yang, Z.; Zhang, F.; Liu, Z.; Yang, P.; Zhang, H.; Yu, B.; Zhao, Y.; Liu, Z. A Rose Bengal-Functionalized Porous Organic Polymer for Carboxylative Cyclization of Propargyl Alcohols with CO₂. *Chem. Commun.* **2019**, *55* (83), 12475–12478.

(68) Jiang, J.-X.; Li, Y.; Wu, X.; Xiao, J.; Adams, D. J.; Cooper, A. I. Conjugated Microporous Polymers with Rose Bengal Dye for Highly Efficient Heterogeneous Organo-Photocatalysis. *Macromolecules* **2013**, *46* (22), 8779–8783.

(69) Liras, M.; Pintado-Sierra, M.; Iglesias, M.; Sánchez, F. A Deprotection Strategy of a BODIPY Conjugated Porous Polymer to Obtain a Heterogeneous (Dipyrrin)(Bipyridine)Ruthenium(II) Visible Light Photocatalyst. *J. Mater. Chem. A* **2016**, *4* (44), 17274–17278.

- (70) Luo, J.; Zhang, X.; Zhang, J. Carbazolic Porous Organic Framework as an Efficient, Metal-Free Visible-Light Photocatalyst for Organic Synthesis. *ACS Catal.* **2015**, *5* (4), 2250–2254.
- (71) Dadashi-Silab, S.; Lorandi, F.; DiTucci, M. J.; Sun, M.; Szczepaniak, G.; Liu, T.; Matyjaszewski, K. Conjugated Cross-Linked Phenothiazines as Green or Red Light Heterogeneous Photocatalysts for Copper-Catalyzed Atom Transfer Radical Polymerization. *J. Am. Chem. Soc.* **2021**, *143* (25), 9630–9638.
- (72) Wang, Z. J.; Garth, K.; Ghasimi, S.; Landfester, K.; Zhang, K. A. I. Conjugated Microporous Poly(Benzochalcogenadiazole)s for Photocatalytic Oxidative Coupling of Amines under Visible Light. *ChemSusChem* **2015**, *8* (20), 3459–3464.
- (73) Battula, V. R.; Singh, H.; Kumar, S.; Bala, I.; Pal, S. K.; Kailasam, K. Natural Sunlight Driven Oxidative Homocoupling of Amines by a Truxene-Based Conjugated Microporous Polymer. *ACS Catal.* **2018**, *8* (8), 6751–6759.
- (74) Wang, Z. J.; Ghasimi, S.; Landfester, K.; Zhang, K. A. I. Molecular Structural Design of Conjugated Microporous Poly-(Benzooxadiazole) Networks for Enhanced Photocatalytic Activity with Visible Light. *Adv. Mater.* **2015**, *27* (40), 6265–6270.
- (75) Su, C.; Tandiana, R.; Tian, B.; Sengupta, A.; Tang, W.; Su, J.; Loh, K. P. Visible-Light Photocatalysis of Aerobic Oxidation Reactions Using Carbazolic Conjugated Microporous Polymers. *ACS Catal.* **2016**, *6* (6), 3594–3599.
- (76) Wang, J.-L.; Wang, C.; deKrafft, K. E.; Lin, W. Cross-Linked Polymers with Exceptionally High Ru(Bipy)₃²⁺ Loadings for Efficient Heterogeneous Photocatalysis. *ACS Catal.* **2012**, *2* (3), 417–424.
- (77) Zhi, Y.; Ma, S.; Xia, H.; Zhang, Y.; Shi, Z.; Mu, Y.; Liu, X. Construction of Donor-Acceptor Type Conjugated Microporous Polymers: A Fascinating Strategy for the Development of Efficient Heterogeneous Photocatalysts in Organic Synthesis. *Appl. Catal. B: Environ.* **2019**, *244*, 36–44.
- (78) Wang, Z. J.; Ghasimi, S.; Landfester, K.; Zhang, K. A. I. A Conjugated Porous Poly-Benzobisthiadiazole Network for a Visible Light-Driven Photoredox Reaction. *J. Mater. Chem. A* **2014**, *2* (44), 18720–18724.
- (79) Lu, M.; Li, Q.; Liu, J.; Zhang, F.-M.; Zhang, L.; Wang, J.-L.; Kang, Z.-H.; Lan, Y.-Q. Installing Earth-Abundant Metal Active Centers to Covalent Organic Frameworks for Efficient Heterogeneous Photocatalytic CO₂ Reduction. *Appl. Catal. B: Environ.* **2019**, *254*, 624–633.
- (80) Wang, L.; Wang, R.; Zhang, X.; Mu, J.; Zhou, Z.; Su, Z. Improved Photoreduction of CO₂ with Water by Tuning the Valence Band of Covalent Organic Frameworks. *ChemSusChem* **2020**, *13* (11), 2973–2980.
- (81) Wan, Y.; Wang, L.; Xu, H.; Wu, X.; Yang, J. A Simple Molecular Design Strategy for Two-Dimensional Covalent Organic Framework Capable of Visible-Light-Driven Water Splitting. *J. Am. Chem. Soc.* **2020**, *142* (9), 4508–4516.
- (82) He, T.; Geng, K.; Jiang, D. Engineering Covalent Organic Frameworks for Light-Driven Hydrogen Production from Water. *ACS Materials Lett.* **2019**, *1* (2), 203–208.
- (83) Chen, J.; Tao, X.; Li, C.; Ma, Y.; Tao, L.; Zheng, D.; Zhu, J.; Li, H.; Li, R.; Yang, Q. Synthesis of Bipyridine-Based Covalent Organic Frameworks for Visible-Light-Driven Photocatalytic Water Oxidation. *Appl. Catal. B: Environ.* **2020**, *262*, No. 118271.
- (84) Chai, S.; Chen, X.; Zhang, X.; Fang, Y.; Sprick, R. S.; Chen, X. Rational Design of Covalent Organic Frameworks for Efficient Photocatalytic Hydrogen Peroxide Production. *Environ. Sci.: Nano* **2022**, *9* (7), 2464–2469.
- (85) Zhao, W.; Yan, P.; Li, B.; Bahri, M.; Liu, L.; Zhou, X.; Clowes, R.; Browning, N. D.; Wu, Y.; Ward, J. W.; Cooper, A. I. Accelerated Synthesis and Discovery of Covalent Organic Framework Photocatalysts for Hydrogen Peroxide Production. *J. Am. Chem. Soc.* **2022**, *144* (22), 9902–9909.
- (86) Li, Q.; Lan, X.; An, G.; Ricardez-Sandoval, L.; Wang, Z.; Bai, G. Visible-Light-Responsive Anthraquinone Functionalized Covalent Organic Frameworks for Metal-Free Selective Oxidation of Sulfides: Effects of Morphology and Structure. *ACS Catal.* **2020**, *10* (12), 6664–6675.
- (87) Hao, W.; Chen, D.; Li, Y.; Yang, Z.; Xing, G.; Li, J.; Chen, L. Facile Synthesis of Porphyrin Based Covalent Organic Frameworks via an A₂B₂ Monomer for Highly Efficient Heterogeneous Catalysis. *Chem. Mater.* **2019**, *31* (19), 8100–8105.
- (88) Basak, A.; Karak, S.; Banerjee, R. Covalent Organic Frameworks as Porous Pigments for Photocatalytic Metal-Free C–H Borylation. *J. Am. Chem. Soc.* **2023**, *145* (13), 7592–7599.
- (89) Wei, P.-F.; Qi, M.-Z.; Wang, Z.-P.; Ding, S.-Y.; Yu, W.; Liu, Q.; Wang, L.-K.; Wang, H.-Z.; An, W.-K.; Wang, W. Benzoxazole-Linked Ultrastable Covalent Organic Frameworks for Photocatalysis. *J. Am. Chem. Soc.* **2018**, *140* (13), 4623–4631.
- (90) Ding, S.-Y.; Gao, J.; Wang, Q.; Zhang, Y.; Song, W.-G.; Su, C.-Y.; Wang, W. Construction of Covalent Organic Framework for Catalysis: Pd/COF-LZU1 in Suzuki–Miyaura Coupling Reaction. *J. Am. Chem. Soc.* **2011**, *133* (49), 19816–19822.
- (91) Chen, H.; Liu, W.; Laemont, A.; Krishnaraj, C.; Feng, X.; Rohman, F.; Meledina, M.; Zhang, Q.; Van Deun, R.; Leus, K.; Van Der Voort, P. A Visible-Light-Harvesting Covalent Organic Framework Bearing Single Nickel Sites as a Highly Efficient Sulfur–Carbon Cross-Coupling Dual Catalyst. *Angew. Chem., Int. Ed.* **2021**, *60* (19), 10820–10827.
- (92) Jati, A.; Dam, S.; Kumar, S.; Kumar, K.; Maji, B. A π -Conjugated Covalent Organic Framework Enables Interlocked Nickel/Photoredox Catalysis for Light-Harvesting Cross-Coupling Reactions. *Chem. Sci.* **2023**, *14* (32), 8624–8634.
- (93) Traxler, M.; Gisbertz, S.; Pachfule, P.; Schmidt, J.; Roeser, J.; Reischauer, S.; Rabeah, J.; Pieber, B.; Thomas, A. Acridine-Functionalized Covalent Organic Frameworks (COFs) as Photocatalysts for Metallaphotocatalytic C–N Cross-Coupling. *Angew. Chem., Int. Ed.* **2022**, *61* (21), No. 17738, DOI: 10.1002/anie.202117738.
- (94) Jati, A.; Dey, K.; Nurhuda, M.; Addicoat, M. A.; Banerjee, R.; Maji, B. Dual Metalation in a Two-Dimensional Covalent Organic Framework for Photocatalytic C–N Cross-Coupling Reactions. *J. Am. Chem. Soc.* **2022**, *144* (17), 7822–7833.
- (95) López-Magano, A.; Ortín-Rubio, B.; Imaz, I.; Maspocho, D.; Alemán, J.; Mas-Ballesté, R. Photoredox Heterobimetallic Dual Catalysis Using Engineered Covalent Organic Frameworks. *ACS Catal.* **2021**, *11* (19), 12344–12354.
- (96) Majumder, P.; Basak, A.; Kuiry, H.; Sasmal, H. S.; Karak, S.; Saha, P.; Chandra, B.; Sen Gupta, S.; Banerjee, R. Proximity-Enabled Photochemical C–H Functionalization Using a Covalent Organic Framework-Confined Fe₂^{IV}– μ -Oxo Species in Water. *J. Am. Chem. Soc.* **2023**, *145* (34), 18855–18864.
- (97) Xia, R.; Overa, S.; Jiao, F. Emerging Electrochemical Processes to Decarbonize the Chemical Industry. *JACS Au* **2022**, *2* (5), 1054–1070.
- (98) Yazdani, A.; Botte, G. G. Perspectives of Electrocatalysis in the Chemical Industry: A Platform for Energy Storage. *Curr. Opin. Chem. Eng.* **2020**, *29*, 89–95.
- (99) Wang, T.; Su, D.; Shanmukaraj, D.; Rojo, T.; Armand, M.; Wang, G. Electrode Materials for Sodium-Ion Batteries: Considerations on Crystal Structures and Sodium Storage Mechanisms. *Electrochem. Energy Rev.* **2018**, *1* (2), 200–237.
- (100) Min, X.; Xiao, J.; Fang, M.; Wang, W.; Zhao, Y.; Liu, Y.; Abdelkader, A. M.; Xi, K.; Kumar, R. V.; Huang, Z. Potassium-Ion Batteries: Outlook on Present and Future Technologies. *Energy Environ. Sci.* **2021**, *14* (4), 2186–2243.
- (101) Ma, L.; Lv, Y.; Wu, J.; Xia, C.; Kang, Q.; Zhang, Y.; Liang, H.; Jin, Z. Recent Advances in Anode Materials for Potassium-Ion Batteries: A Review. *Nano Res.* **2021**, *14* (12), 4442–4470.
- (102) Nayak, P. K.; Yang, L.; Brehm, W.; Adelhelm, P. From Lithium-Ion to Sodium-Ion Batteries: Advantages, Challenges, and Surprises. *Angew. Chem., Int. Ed.* **2018**, *57* (1), 102–120.
- (103) Paris, A. R.; Bocarsly, A. B. High-Efficiency Conversion of CO₂ to Oxalate in Water Is Possible Using a Cr-Ga Oxide Electrocatalyst. *ACS Catal.* **2019**, *9* (3), 2324–2333.

- (104) Blanco, D. E.; Atwi, R.; Sethuraman, S.; Lasri, A.; Morales, J.; Rajput, N. N.; Modestino, M. A. Effect of Electrolyte Cations on Organic Electrosynthesis: The Case of Adiponitrile Electrochemical Production. *J. Electrochem. Soc.* **2020**, *167* (15), 155526.
- (105) Ciancaleoni, G.; Belpassi, L.; Zuccaccia, D.; Tarantelli, F.; Belanzoni, P. Counterion Effect in the Reaction Mechanism of NHC Gold(I)-Catalyzed Alkoxylation of Alkynes: Computational Insight into Experiment. *ACS Catal.* **2015**, *5* (2), 803–814.
- (106) Nitopi, S.; Bertheussen, E.; Scott, S. B.; Liu, X.; Engstfeld, A. K.; Horch, S.; Seger, B.; Stephens, I. E. L.; Chan, K.; Hahn, C.; Nørskov, J. K.; Jaramillo, T. F.; Chorkendorff, I. Progress and Perspectives of Electrochemical CO₂ Reduction on Copper in Aqueous Electrolyte. *Chem. Rev.* **2019**, *119* (12), 7610–7672.
- (107) Cronin, S. P.; Dulovic, S.; Lawrence, J. A.; Filsinger, K. A.; Hernandez-Gonzalez, A. P.; Evans, R.; Stiles, J. W.; Morris, J.; Pelczer, I.; Bocarsly, A. B. Direct Synthesis of 1-Butanol with High Faradaic Efficiency from CO₂ Utilizing Cascade Catalysis at a Ni-Enhanced (Cr₂O₃)₃Ga₂O₃ Electrocatalyst. *J. Am. Chem. Soc.* **2023**, *145* (12), 6762–6772.
- (108) White, J. L.; Baruch, M. F.; Pander, J. E.; Hu, Y.; Fortmeyer, I. C.; Park, J. E.; Zhang, T.; Liao, K.; Gu, J.; Yan, Y.; Shaw, T. W.; Abelev, E.; Bocarsly, A. B. Light-Driven Heterogeneous Reduction of Carbon Dioxide: Photocatalysts and Photoelectrodes. *Chem. Rev.* **2015**, *115* (23), 12888–12935.
- (109) Masias, A.; Marcicki, J.; Paxton, W. A. Opportunities and Challenges of Lithium Ion Batteries in Automotive Applications. *ACS Energy Letters* **2021**, *6* (2), 621–630.
- (110) Dhir, S.; Wheeler, S.; Capone, I.; Pasta, M. Outlook on K-Ion Batteries. *Chem.* **2020**, *6* (10), 2442–2460.
- (111) Janoschka, T.; Hager, M. D.; Schubert, U. S. Powering up the Future: Radical Polymers for Battery Applications. *Adv. Mater.* **2012**, *24* (48), 6397–6409.
- (112) Lu, Y.; Chen, J. Prospects of Organic Electrode Materials for Practical Lithium Batteries. *Nat. Rev. Chem.* **2020**, *4* (3), 127–142.
- (113) Heiska, J.; Nisula, M.; Karppinen, M. Organic Electrode Materials with Solid-State Battery Technology. *J. Mater. Chem. A* **2019**, *7* (32), 18735–18758.
- (114) Haldar, S.; Schneemann, A.; Kaskel, S. Covalent Organic Frameworks as Model Materials for Fundamental and Mechanistic Understanding of Organic Battery Design Principles. *J. Am. Chem. Soc.* **2023**, *145* (25), 13494–13513.
- (115) Kim, J.; Shirke, Y.; Milner, P. J. Flexible Backbone Effects on the Redox Properties of Peryleneimide-Based Polymers. *ACS Appl. Mater. Interfaces* **2023**, DOI: 10.1021/acsmi.3c06065.
- (116) Peterson, B. M.; Gannett, C. N.; Melecio-Zambrano, L.; Fors, B. P.; Abruña, H. Effect of Structural Ordering on the Charge Storage Mechanism of p-Type Organic Electrode Materials. *ACS Appl. Mater. Interfaces* **2021**, *13* (6), 7135–7141.
- (117) Tang, M.; Zhu, S.; Liu, Z.; Jiang, C.; Wu, Y.; Li, H.; Wang, B.; Wang, E.; Ma, J.; Wang, C. Tailoring π -Conjugated Systems: From π - π Stacking to High-Rate-Performance Organic Cathodes. *Chem.* **2018**, *4* (11), 2600–2614.
- (118) Wang, H.-G.; Yuan, S.; Ma, D.-L.; Huang, X.-L.; Meng, F.-L.; Zhang, X.-B. Tailored Aromatic Carbonyl Derivative Polyimides for High-Power and Long-Cycle Sodium-Organic Batteries. *Adv. Energy Mater.* **2014**, *4* (7), No. 1301651.
- (119) Xie, J.; Zhang, Q. Recent Progress in Multivalent Metal (Mg, Zn, Ca, and Al) and Metal-Ion Rechargeable Batteries with Organic Materials as Promising Electrodes. *Small* **2019**, *15* (15), No. 1805061.
- (120) Obrezkov, F. A.; Shestakov, A. F.; Traven, V. F.; Stevenson, K. J.; Troshin, P. A. An Ultrafast Charging Polyphenylamine-Based Cathode Material for High Rate Lithium, Sodium and Potassium Batteries. *J. Mater. Chem. A* **2019**, *7* (18), 11430–11437.
- (121) Kato, M.; Masese, T.; Yao, M.; Takeichi, N.; Kiyobayashi, T. Organic Positive-Electrode Material Utilizing Both an Anion and Cation: A Benzoquinone-Tetrathiafulvalene Triad Molecule, Q-TTF-Q, for Rechargeable Li, Na, and K Batteries. *New J. Chem.* **2019**, *43* (3), 1626–1631.
- (122) Gannett, C. N.; Peterson, B. M.; Shen, L.; Seok, J.; Fors, B. P.; Abruña, H. D. Cross-Linking Effects on Performance Metrics of Phenazine-Based Polymer Cathodes. *ChemSusChem* **2020**, *13*, 2428–2435.
- (123) Song, Z.; Qian, Y.; Gordin, M. L.; Tang, D.; Xu, T.; Otani, M.; Zhan, H.; Zhou, H.; Wang, D. Polyanthraquinone as a Reliable Organic Electrode for Stable and Fast Lithium Storage. *Angew. Chem., Int. Ed.* **2015**, *54* (47), 13947–13951.
- (124) Paris, A. R.; Bocarsly, A. B. Ni-Al Films on Glassy Carbon Electrodes Generate an Array of Oxygenated Organics from CO₂. *ACS Catal.* **2017**, *7* (10), 6815–6820.
- (125) Rodríguez-Calero, G. G.; Conte, S.; Lowe, M. A.; Burkhardt, S. E.; Gao, J.; John, J.; Hernández-Burgos, K.; Abruña, H. D. *In Situ* Electrochemical Characterization of Poly-3,4-Ethylenedioxythiophene/Tetraalkylphenylene Diamine Films and Their Potential Use in Electrochemical Energy Storage Devices. *J. Electroanal. Chem.* **2016**, *765*, 65–72.
- (126) Seok, J.; Gannett, C. N.; Yu, S. H.; Abruña, H. D. Understanding the Impacts of Li Stripping Overpotentials at the Counter Electrode by Three-Electrode Coin Cell Measurements. *Anal. Chem.* **2021**, *93* (46), 15459–15467.
- (127) Wu, X.; Gannett, C. N.; Liu, J.; Zeng, R.; Novaes, L. F. T.; Wang, H.; Abruña, H. D.; Lin, S. Intercepting Hydrogen Evolution with Hydrogen-Atom Transfer: Electron-Initiated Hydrofunctionalization of Alkenes. *J. Am. Chem. Soc.* **2022**, *144* (39), 17783–17791.
- (128) Cong, C.; Kim, J.; Gannett, C. N.; Abruña, H. D.; Milner, P. J. Unexpected Direct Synthesis of Tunable Redox-Active Benzil-Linked Polymers via the Benzoin Reaction. *ACS Appl. Polym. Mater.* **2023**, *5* (1), 1056–1066.
- (129) Kuo, H.-Y.; Lee, T. S.; Chu, A. T.; Tignor, S. E.; Scholes, G. D.; Bocarsly, A. B. A Cyanide-Bridged Di-Manganese Carbonyl Complex That Photochemically Reduces CO₂ to CO. *Dalton Trans.* **2019**, *48* (4), 1226–1236.
- (130) Kim, T.; Choi, W.; Shin, H.-C.; Choi, J.-Y.; Kim, J. M.; Park, M.-S.; Yoon, W.-S. Applications of Voltammetry in Lithium Ion Battery Research. *J. Electrochem. Sci. Technol.* **2020**, *11* (1), 14–25.
- (131) Levi, M. D.; Aurbach, D. The Mechanism of Lithium Intercalation in Graphite Film Electrodes in Aprotic Media. Part 1. High Resolution Slow Scan Rate Cyclic Voltammetric Studies and Modeling. *J. Electroanal. Chem.* **1997**, *421* (1–2), 79–88.
- (132) Wang, B.; Aoki, K. J.; Chen, J.; Nishiumi, T. Slow Scan Voltammetry for Diffusion-Controlled Currents in Sodium Alginate Solutions. *J. Electroanal. Chem.* **2013**, *700*, 60–64.
- (133) Acker, P.; Rzesny, L.; Marchiori, C. F. N.; Araujo, C. M.; Esser, B. π -Conjugation Enables Ultra-High Rate Capabilities and Cycling Stabilities in Phenothiazine Copolymers as Cathode-Active Battery Materials. *Adv. Funct. Mater.* **2019**, *29* (45), No. 1906436.
- (134) Lukatskaya, M. R.; Dunn, B.; Gogotsi, Y. Multidimensional Materials and Device Architectures for Future Hybrid Energy Storage. *Nat. Commun.* **2016**, *7* (1), 1–13.
- (135) Ji, X. A Paradigm of Storage Batteries. *Energy Environ. Sci.* **2019**, *12* (11), 3203–3224.
- (136) Wu, X.; Markir, A.; Ma, L.; Xu, Y.; Jiang, H.; Leonard, D. P.; Shin, W.; Wu, T.; Lu, J.; Ji, X. A Four-Electron Sulfur Electrode Hosting a Cu²⁺/Cu⁺ Redox Charge Carrier. *Angew. Chem., Int. Ed.* **2019**, *58* (36), 12640–12645.
- (137) Wang, H.; He, J.; Liu, J.; Qi, S.; Wu, M.; Wen, J.; Chen, Y.; Feng, Y.; Ma, J. Electrolytes Enriched by Crown Ethers for Lithium Metal Batteries. *Adv. Funct. Materials.* **2021**, *31* (2), No. 2002578.
- (138) Yang, Y.-F.; Chiou, C.-Y.; Liu, C.-W.; Chen, C.-L.; Lee, J.-T. Crown Ethers as Electrolyte Additives To Modulate the Electrochemical Potential of Lithium Organic Batteries. *J. Phys. Chem. C* **2019**, *123* (36), 21950–21958.
- (139) Zhao, H.; Qi, J.; Tang, X.; Zhang, K.; Teng, J.; Ding, H.; Tao, Q.; Li, J. Effect of Crown Ether Additive on the Compatibility of Electrolyte and Hard Carbon Anode in Sodium Ion Battery. *J. Alloys Compd.* **2023**, *948*, No. 169823.
- (140) Khurana, R.; Schaefer, J. L.; Archer, L. A.; Coates, G. W. Suppression of Lithium Dendrite Growth Using Cross-Linked

- Polyethylene/Poly(Ethylene Oxide) Electrolytes: A New Approach for Practical Lithium-Metal Polymer Batteries. *J. Am. Chem. Soc.* **2014**, *136* (20), 7395–7402.
- (141) Zhu, Z.; Hong, M.; Guo, D.; Shi, J.; Tao, Z.; Chen, J. All-Solid-State Lithium Organic Battery with Composite Polymer Electrolyte and Pillar[5]Quinone Cathode. *J. Am. Chem. Soc.* **2014**, *136* (47), 16461–16464.
- (142) Jiang, S.; Li, W.; Xie, Y.; Yan, X.; Zhang, K.; Jia, Z. An All-Organic Battery with 2.8 V Output Voltage. *Chem. Eng. J.* **2022**, *434*, No. 134651.
- (143) Verma, A.; Smith, K.; Santhanagopalan, S.; Abraham, D.; Yao, K. P.; Mukherjee, P. P. Galvanostatic Intermittent Titration and Performance Based Analysis of $\text{LiNi}_{0.5}\text{Co}_{0.2}\text{Mn}_{0.3}\text{O}_2$ Cathode. *J. Electrochem. Soc.* **2017**, *164* (13), A3380–A3392.
- (144) Shpigel, N.; Levi, M. D.; Aurbach, D. EQCM-D Technique for Complex Mechanical Characterization of Energy Storage Electrodes: Background and Practical Guide. *Energy Storage Mater.* **2019**, *21*, 399–413.
- (145) Weidlich, C.; Mangold, K.-M.; Jüttner, K. EQCM Study of the Ion Exchange Behaviour of Polypyrrole with Different Counterions in Different Electrolytes. *Electrochim. Acta* **2005**, *50* (7–8), 1547–1552.
- (146) Thakur, R. M.; Easley, A. D.; Wang, S.; Zhang, Y.; Ober, C. K.; Lutkenhaus, J. L. Real Time Quantification of Mixed Ion and Electron Transfer Associated with the Doping of Poly(3-Hexylthiophene). *J. Mater. Chem. C* **2022**, *10* (18), 7251–7262.
- (147) Vitaku, E.; Gannett, C. N.; Carpenter, K. L.; Shen, L.; Abruña, H. D.; Dichtel, W. R. Phenazine-Based Covalent Organic Framework Cathode Materials with High Energy and Power Densities. *J. Am. Chem. Soc.* **2020**, *142* (1), 16–20.
- (148) Yang, Y.; Xiong, Y.; Zeng, R.; Lu, X.; Krumov, M.; Huang, X.; Xu, W.; Wang, H.; DiSalvo, F. J.; Brock, J. D.; Muller, D. A.; Abruña, H. D. *Operando* Methods in Electrocatalysis. *ACS Catal.* **2021**, *11* (3), 1136–1178.
- (149) Zhai, Y.; Zhu, Z.; Zhou, S.; Zhu, C.; Dong, S. Recent Advances in Spectroelectrochemistry. *Nanoscale* **2018**, *10* (7), 3089–3111.
- (150) Gourdin, G.; Doan-Nguyen, V. *In Situ, Operando* Characterization of Materials for Electrochemical Devices. *Cell Rep. Phys. Sci.* **2021**, *2* (12), No. 100660.
- (151) Strauss, F.; Kitsche, D.; Ma, Y.; Teo, J. H.; Goonetilleke, D.; Janek, J.; Bianchini, M.; Brezesinski, T. *Operando* Characterization Techniques for All-Solid-State Lithium-Ion Batteries. *Adv. Energy Sustain. Res.* **2021**, *2* (6), No. 2100004.
- (152) Lin, X.-M.; Yang, X.-T.; Chen, H.-N.; Deng, Y.-L.; Chen, W.-H.; Dong, J.-C.; Wei, Y.-M.; Li, J.-F. *In Situ* Characterizations of Advanced Electrode Materials for Sodium-Ion Batteries toward High Electrochemical Performances. *J. Energy Chem.* **2023**, *76*, 146–164.
- (153) Chen, Y.; Dai, H.; Fan, K.; Zhang, G.; Tang, M.; Gao, Y.; Zhang, C.; Guan, L.; Mao, M.; Liu, H.; Zhai, T.; Wang, C. A Recyclable and Scalable High-Capacity Organic Battery. *Angew. Chem., Int. Ed.* **2023**, *62* (27), No. e202302539.
- (154) Tang, M.; Jiang, C.; Liu, S.; Li, X.; Chen, Y.; Wu, Y.; Ma, J.; Wang, C. Small Amount COFs Enhancing Storage of Large Anions. *Energy Storage Mater.* **2020**, *27*, 35–42.
- (155) Shi, R.; Liu, L.; Lu, Y.; Wang, C.; Li, Y.; Li, L.; Yan, Z.; Chen, J. Nitrogen-Rich Covalent Organic Frameworks with Multiple Carbonyls for High-Performance Sodium Batteries. *Nat. Commun.* **2020**, *11* (1), No. 178.
- (156) Lin, X.-M.; Wu, D.-Y.; Gao, P.; Chen, Z.; Ruben, M.; Fichtner, M. Monitoring the Electrochemical Energy Storage Processes of an Organic Full Rechargeable Battery via *Operando* Raman Spectroscopy: A Mechanistic Study. *Chem. Mater.* **2019**, *31* (9), 3239–3247.
- (157) Peng, C.; Ning, G.-H.; Su, J.; Zhong, G.; Tang, W.; Tian, B.; Su, C.; Yu, D.; Zu, L.; Yang, J.; Ng, M.-F.; Hu, Y.-S.; Yang, Y.; Armand, M.; Loh, K. P. Reversible Multi-Electron Redox Chemistry of π -Conjugated N-Containing Heteroaromatic Molecule-Based Organic Cathodes. *Nat. Energy* **2017**, *2* (7), No. 17074.
- (158) Shestakov, A. F.; Yarmolenko, O. V.; Ignatova, A. A.; Mummyatov, A. V.; Stevenson, K. J.; Troshin, P. A. Structural Origins of Capacity Fading in Lithium-Polyimide Batteries. *J. Mater. Chem. A* **2017**, *5* (14), 6532–6537.
- (159) Raciti, D.; Wang, C. Recent Advances in CO_2 Reduction Electrocatalysis on Copper. *ACS Energy Lett.* **2018**, *3* (7), 1545–1556.
- (160) He, J.; Johnson, N. J. J.; Huang, A.; Berlinguette, C. P. Electrocatalytic Alloys for CO_2 Reduction. *ChemSusChem* **2018**, *11* (1), 48–57.
- (161) Zhang, S.; Fan, Q.; Xia, R.; Meyer, T. J. CO_2 Reduction: From Homogeneous to Heterogeneous Electrocatalysis. *Acc. Chem. Res.* **2020**, *53* (1), 255–264.
- (162) Wang, Y.; Han, P.; Lv, X.; Zhang, L.; Zheng, G. Defect and Interface Engineering for Aqueous Electrocatalytic CO_2 Reduction. *Joule* **2018**, *2* (12), 2551–2582.
- (163) Sun, Z.; Ma, T.; Tao, H.; Fan, Q.; Han, B. Fundamentals and Challenges of Electrochemical CO_2 Reduction Using Two-Dimensional Materials. *Chem.* **2017**, *3* (4), 560–587.
- (164) Cai, X.; Liu, H.; Wei, X.; Yin, Z.; Chu, J.; Tang, M.; Zhuang, L.; Deng, H. Molecularly Defined Interface Created by Porous Polymeric Networks on Gold Surface for Concerted and Selective CO_2 Reduction. *ACS Sustain. Chem. Eng.* **2018**, *6* (12), 17277–17283.
- (165) Zhu, H.-J.; Lu, M.; Wang, Y.-R.; Yao, S.-J.; Zhang, M.; Kan, Y.-H.; Liu, J.; Chen, Y.; Li, S.-L.; Lan, Y.-Q. Efficient Electron Transmission in Covalent Organic Framework Nanosheets for Highly Active Electrocatalytic Carbon Dioxide Reduction. *Nat. Commun.* **2020**, *11* (1), No. 497.
- (166) Lin, R.-B.; Chen, B. Reducing CO_2 with Stable Covalent Organic Frameworks. *Joule* **2018**, *2* (6), 1030–1032.
- (167) Liu, H.; Chu, J.; Yin, Z.; Cai, X.; Zhuang, L.; Deng, H. Covalent Organic Frameworks Linked by Amine Bonding for Concerted Electrochemical Reduction of CO_2 . *Chem.* **2018**, *4* (7), 1696–1709.
- (168) Jin, S.; Hao, Z.; Zhang, K.; Yan, Z.; Chen, J. Advances and Challenges for the Electrochemical Reduction of CO_2 to CO: From Fundamentals to Industrialization. *Angew. Chem., Int. Ed.* **2021**, *60* (38), 20627–20648.
- (169) Nutting, J. E.; Rafiee, M.; Stahl, S. S. Tetramethylpiperidine *N*-Oxyl (TEMPO), Phthalimide *N*-Oxyl (PINO), and Related *N*-Oxyl Species: Electrochemical Properties and Their Use in Electrocatalytic Reactions. *Chem. Rev.* **2018**, *118* (9), 4834–4885.
- (170) Wang, F.; Stahl, S. S. Electrochemical Oxidation of Organic Molecules at Lower Overpotential: Accessing Broader Functional Group Compatibility with Electron–Proton Transfer Mediators. *Acc. Chem. Res.* **2020**, *53* (3), 561–574.
- (171) Savéant, J.-M. Molecular Catalysis of Electrochemical Reactions. Mechanistic Aspects. *Chem. Rev.* **2008**, *108* (7), 2348–2378.
- (172) Das, A.; Stahl, S. S. Noncovalent Immobilization of Molecular Electrocatalysts for Chemical Synthesis: Efficient Electrochemical Alcohol Oxidation with a Pyrene–TEMPO Conjugate. *Angew. Chem., Int. Ed.* **2017**, *56* (30), 8892–8897.
- (173) Hickey, D. P.; Milton, R. D.; Chen, D.; Sigman, M. S.; Minter, S. D. TEMPO-Modified Linear Poly(Ethylenimine) for Immobilization-Enhanced Electrocatalytic Oxidation of Alcohols. *ACS Catal.* **2015**, *5* (9), 5519–5524.
- (174) Yang, L.; Cao, L.; Huang, R.; Hou, Z.-W.; Qian, X.-Y.; An, B.; Xu, H.-C.; Lin, W.; Wang, C. Two-Dimensional Metal–Organic Layers on Carbon Nanotubes to Overcome Conductivity Constraint in Electrocatalysis. *ACS Appl. Mater. Interfaces* **2018**, *10* (42), 36290–36296.